

# High energy (photo) electron spectroscopy

George Sawatzky

UBC Vancouver

# Summary

- A few examples of successes in  
Hard X-Ray photoemission  
Laser based low energy photoemission  
Angular resolved UV photoemission
- New: surfaces and buried interfaces of ionic correlated electron system can Hard x ray photoemission compete with resonant x ray scattering -pros and cons and complimentarity

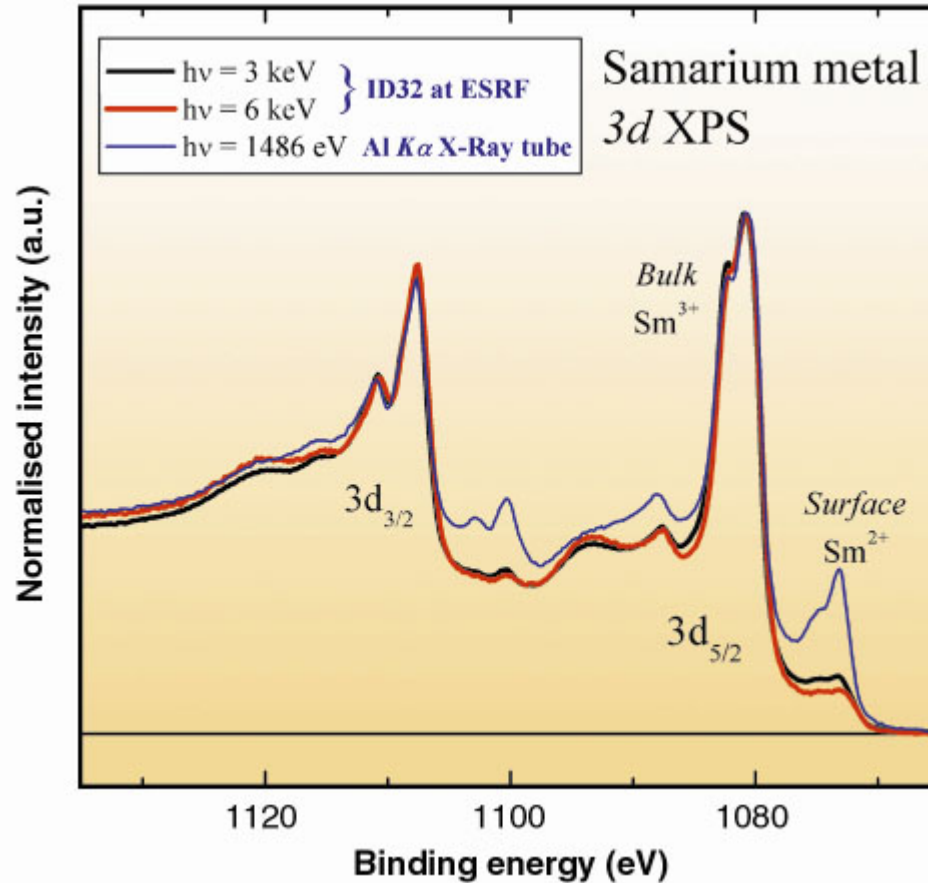
# Hard X Ray has many great successes but there are also issues

- One has demonstrated in many examples the strong differences in surface and bulk electronic structure ( Kondo lattice, rare earths, transition metal oxides, Ca-SrVo<sub>3</sub>, V<sub>2</sub>O<sub>3</sub>--- has kept theory like DMFT honest).

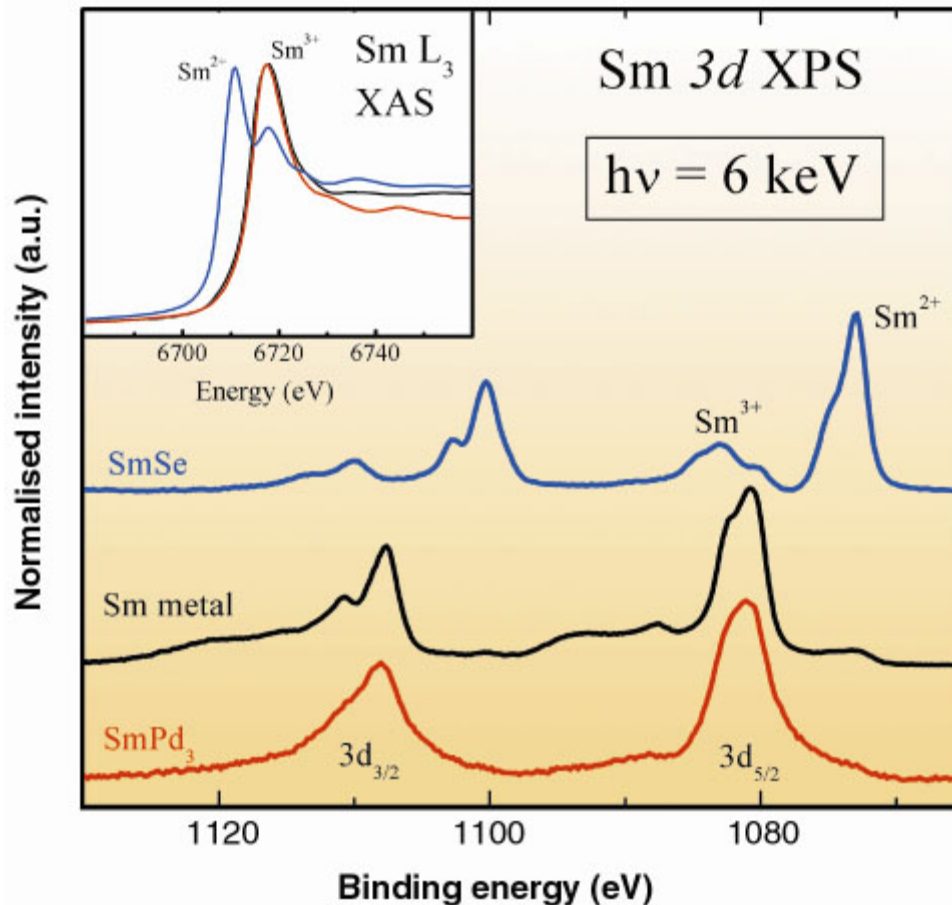
# Issues at higher energies are

- Inferior Energy resolution,
- difficult to get high momentum resolution
- cross section decrease rapidly with energy
- must take into account recoil energy and momentum
- transitions are no longer dipole only.

C. Dallera , L. Duò , G. Panaccione , G. Paolicelli L. Braicovich and A. Palenzona .



Photoemission spectra of 3d levels in pure metallic samarium. Spectra at 3 and 6 keV were measured at ID32 while the spectrum excited at 1486 eV was taken with an X-ray tube. A relevant decrease of the divalent surface component with increasing energy is seen.



Photoemission spectra of samarium 3d levels in three samples with different weight of the divalent and trivalent component in bulk and surface, after background subtraction. The L<sub>3</sub> edge absorption spectra (inset) show less structure

**Kondo lattice effects and the collapse of lattice coherence in  $\text{Yb}_{1-x}\text{Lu}_x\text{B}_{12}$  studied by hard x-ray photoelectron spectroscopy**  
 J. Yamaguchi, -----S. Suga

PHYSICAL REVIEW B 79, 125121 (2009)

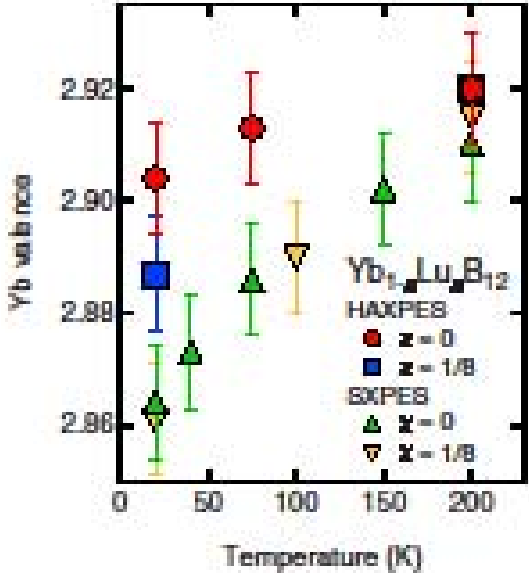


FIG. 3. (Color online)  $T$  dependence of the Yb valence estimated from the Yb 3d HAXPES ( $h\nu \sim 8$  keV) and Yb 4f SXPES ( $h\nu = 700$  eV) (Ref. 41) spectra of  $\text{Yb}_{1-x}\text{Lu}_x\text{B}_{12}$  ( $x=0$  and  $1/8$ ).

Fig. 3. For comparison, the Yb valence estimated from the

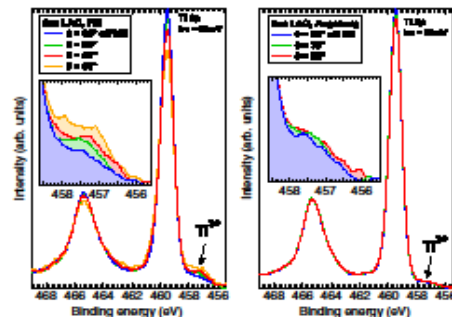


FIG. 1 (color online). Ti 2*p* spectra of two different LAO/STO samples for various emission angles  $\theta$ .

photons amounted to  $\approx 500$  meV. Binding energies were calibrated with reference to the Au 4*f* core level at 84.0 eV. Because of the large probing depth, no particular surface preparation was necessary. The Augsburg 4 uc sample has been contacted as described in Ref. [8] and allowed for *in situ* conductivity measurements. All data were recorded at RT and were normalized to the background intensity at higher binding energies or, equivalently, to equal integrated intensity.

In Fig. 1, HAXPES spectra are presented of the Ti 2*p* doublet at different emission angles  $\theta$  with respect to the surface normal (normal emission—NE). The data sets were recorded on PSI (left panel) and Augsburg (right panel) samples exhibiting an interface 2DEG. The low spectral weight at the lower binding energy side of the main line, detailed in the insets in Fig. 1, can be attributed to emission from the 2*p* level of  $\text{Ti}^{3+}$  as evidenced by its energetic shift of 2.2 eV. Thus it represents a direct manifestation of additional electrons hosted in the otherwise empty 3*d* shell of  $\text{Ti}^{4+}$  in STO. We note that this has not been seen before with soft x-ray PES due to the insufficient probing depth [12]. By going to larger emission angles—which corresponds to a decrease in the effective electron escape depth as  $\lambda_{\text{eff}} = \lambda \cos\theta$  (see Fig. 2)—the  $\text{Ti}^{3+}$  signal increases in relation to the  $\text{Ti}^{4+}$  main line. From these observations we deduce that the extra electrons are localized at the STO side of the LAO/STO interface within a region considerably smaller than the electron escape depth.

For a more quantitative analysis we use the following simple model (cf. Fig. 2): The 2DEG extends from the interface to a depth  $d$  into the STO substrate. The interface region is stoichiometric and characterized by a constant fraction  $p$  of  $\text{Ti}^{3+}$  ions per unit cell. Taking into account the exponential damping factor  $e^{-z/\lambda_{\text{eff}}}$  for photoelectrons created in depth  $z$ , one can easily calculate the ratio of  $\text{Ti}^{3+}$  to  $\text{Ti}^{4+}$  signal as a function of emission angle  $\theta$  (note that

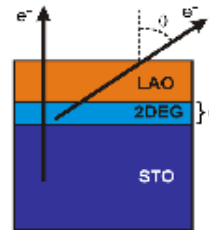


FIG. 2 (color online). Schematic illustrating depth profiling by angle-dependent HAXPES.

the damping in the LAO overlayer does not change this ratio anymore but only results in an absolute reduction of the signal):

$$\frac{I(3+)}{I(4+)} = \frac{p[1 - \exp(-d/\lambda \cos\theta)]}{1 - p[1 - \exp(-d/\lambda \cos\theta)]}. \quad (1)$$

For  $d \gg \lambda$ , Eq. (1) reduces to  $I(3+)/I(4+) = p/(1-p)$ , which means that there is no angular dependence in this case. Note that in Eq. (1)  $p$  and  $d$  are not independent. However, due to the exponentials  $d$  reacts very sensitively to a small variation of  $p$  except in the limit  $d \ll \lambda$ , implying that the parameter range for  $p$  and  $d$  can be narrowed effectively by comparison with experiment.

This is illustrated in Fig. 3, where we show the angle dependence of the  $I(3+)/I(4+)$  ratio for several LAO/STO samples, as obtained by a standard fitting procedure. The shaded areas mark the array of curves according to Eq. (1) falling within the error bars ( $\pm 20\%$ ) of the experimental  $I(3+)/I(4+)$  ratios. The corresponding parameter ranges for  $p$  and  $d$  are indicated in Fig. 3 and listed in Table I for all samples. Also drawn are best fit curves (solid lines). The electron escape depth  $\lambda$  in STO was fixed to 40 Å according to the NIST database [18] and experimental findings on other insulating oxide compounds [19–21]. As can be seen

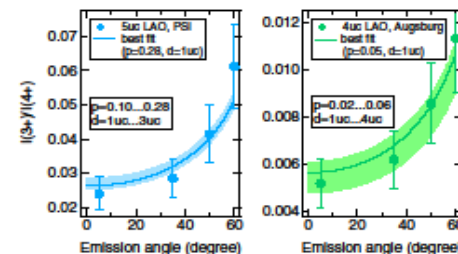


FIG. 3 (color online). Experimental  $I(3+)/I(4+)$  ratios for two LAO/STO samples as a function of angle.

Profiling the Interface Electron Gas of  $\text{LaAlO}_3\text{-SrTiO}_3$   
*Heterostructures*  
 with Hard X-Ray Photoelectron Spectroscopy  
 M. Sing,<sup>1</sup> et al

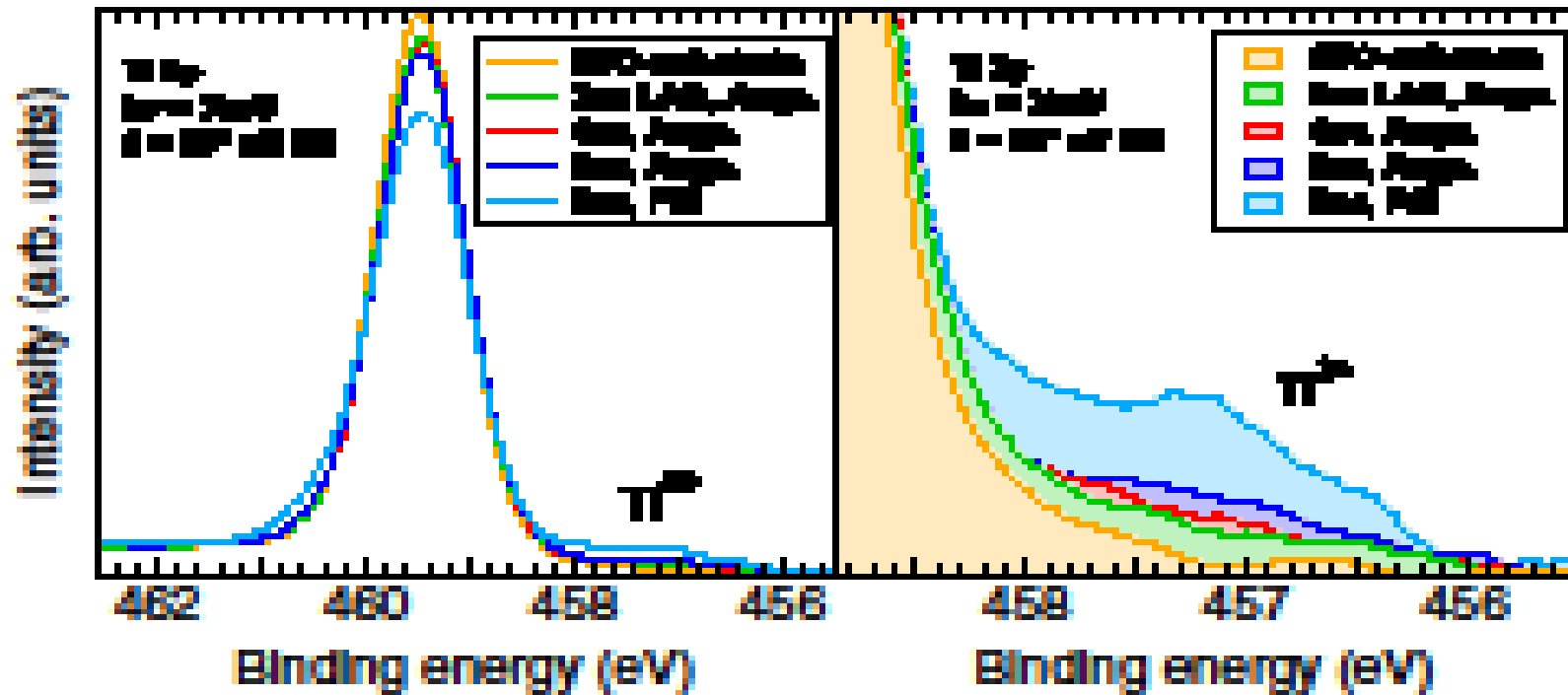


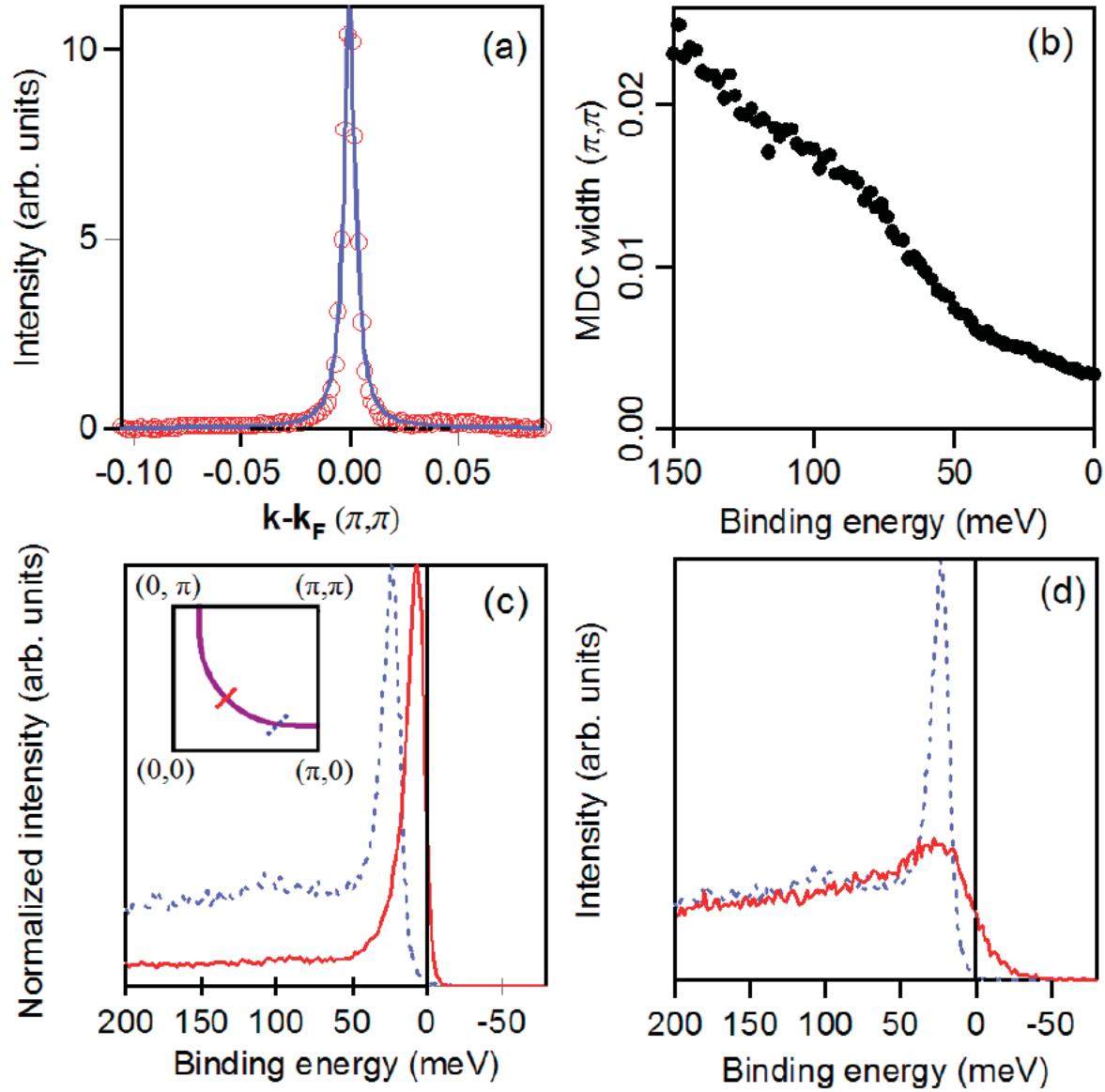
FIG. 4 (color online).  $\text{Ti } 2p$  spectra of various samples plus bare STO at a fixed emission angle.

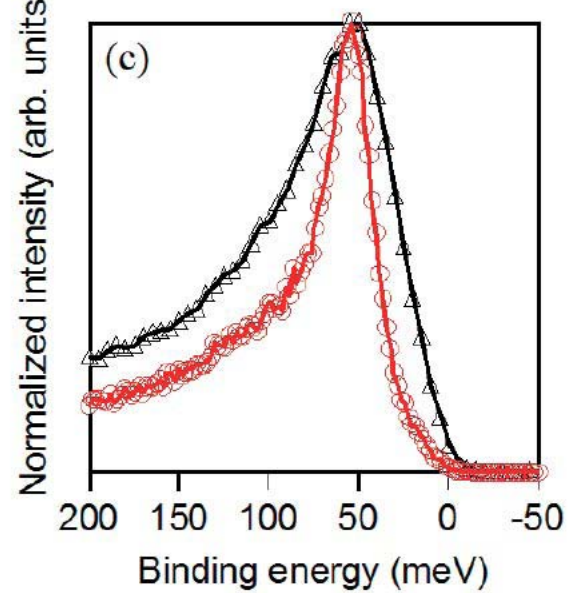
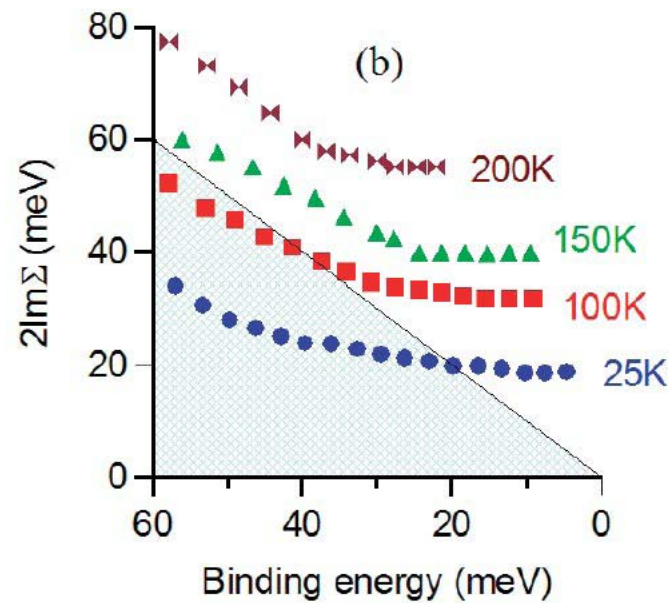
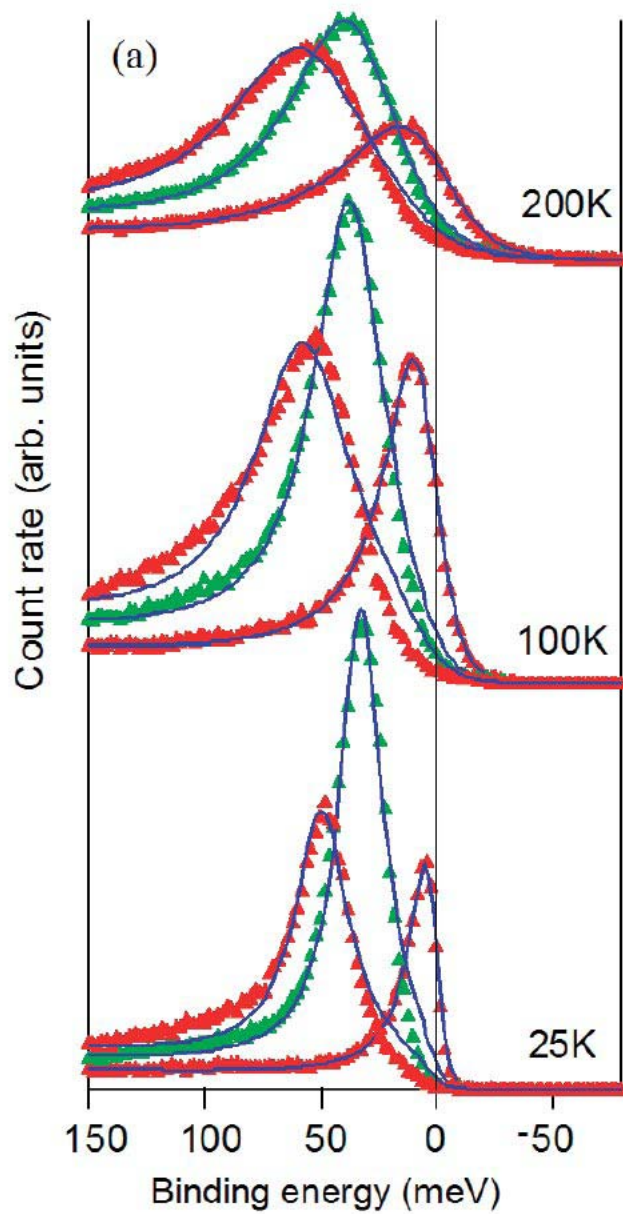
# Laser low energy photoemission

- The escape depth is also quite large i.e. bulk sensitive
- But it varies strongly from compound to compound i.e.  $\epsilon(q, \omega)$  is strongly material dependent at low energy
- The energy resolution is exceptional
- Severe problem with finding final states with energy and momentum conservation ( band structure effects).
- Inhomogeneous work function can strongly affect the spectrum

# Laser Based Angle-Resolved Photoemission, the Sudden Approximation, and Quasiparticle-Like Spectral Peaks in $\text{Bi}_2\text{Sr}_2\text{CaCu}_2\text{O}_8$

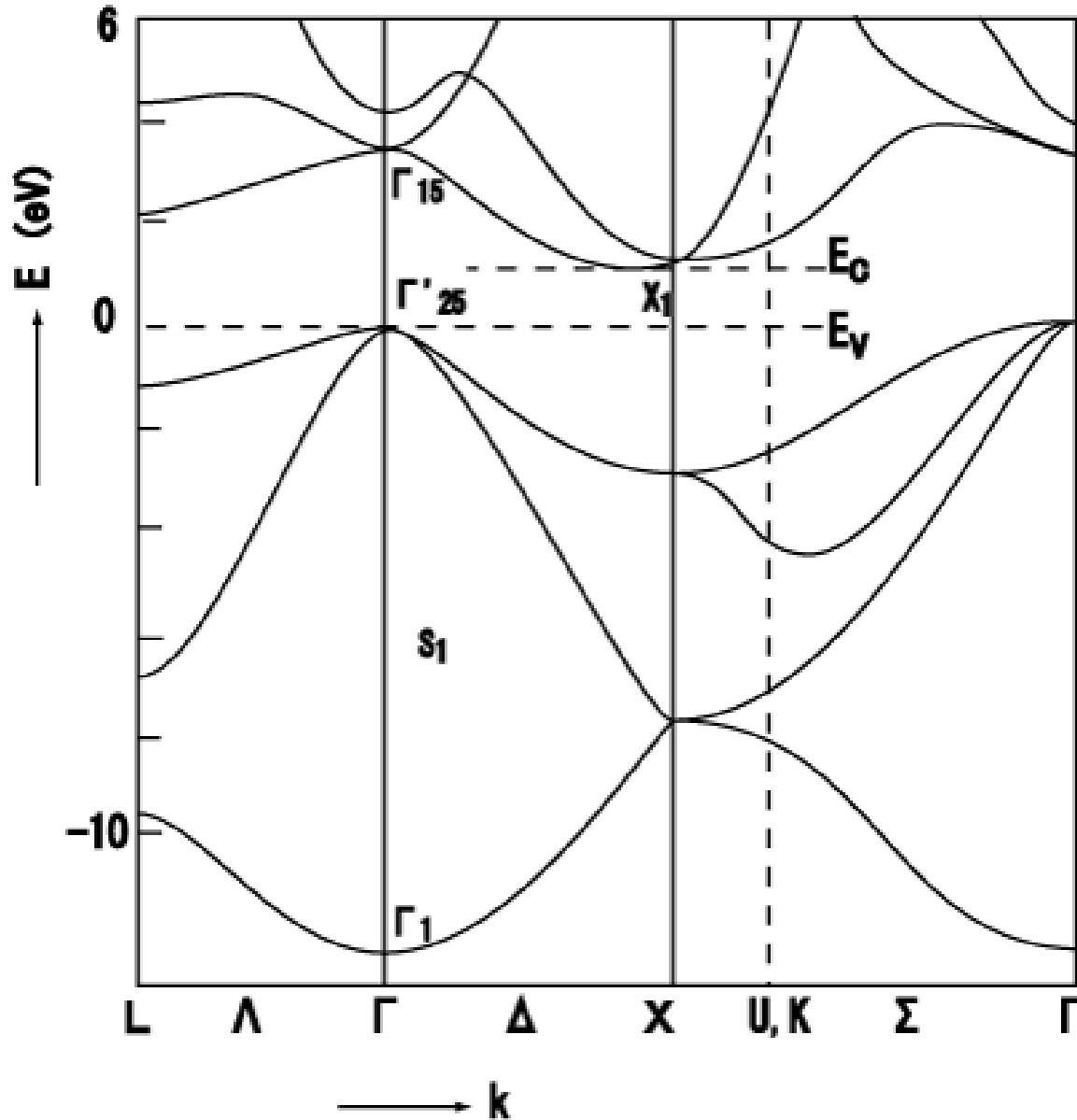
Dessau group PRL 96, 017005 (2006)  
PHYSICAL REVIEW LETTERS 2006





Can we reach final states??

## Band structure of Si



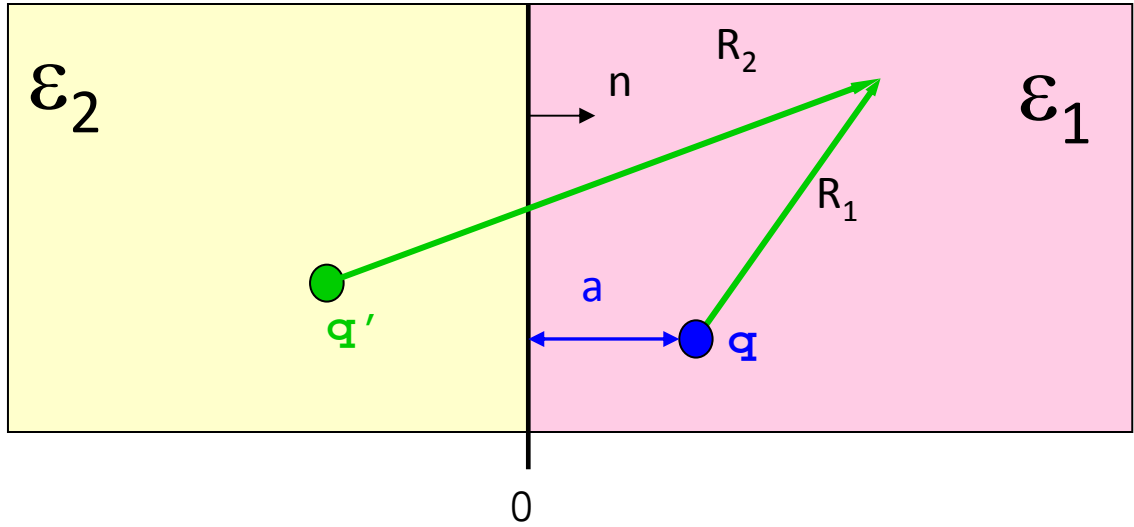
# ARPES at UV photon energies

- Spectacular high energy and momentum resolution for 2D systems ( High  $T_c$ 's, Graphene,-----)
- Strongly surface sensitive. Don't know what to do with  $K_z$
- Very important for surface states and ultra thin films

There are many important results from all of these spectroscopies. What about their application to surface of ionic materials and buried interfaces?

# Potential of a point charge in the neighbourhood of a dielectric

Macroscopic continuum - uniform



$$(D_1 - D_2) \cdot n = 4\pi\sigma$$

$$(E_1 - E_2) \times n = 0$$

$\sigma$  - surface charge

$$\epsilon_1 \nabla \cdot E = 4\pi \cdot l \quad z > 0$$

$$\epsilon_2 \nabla \cdot E = 0 \quad z < 0$$

$$\nabla \times E = 0$$

$$\phi = \frac{1}{\epsilon_1} \left( \frac{q}{R_1} + \frac{q'}{R_2} \right)$$

$$q' = - \frac{(\epsilon_2 - \epsilon_1)}{(\epsilon_2 + \epsilon_1)} q$$

Energy to create a charge  $q$  at  $a$  :

$$E = - \int_0^Q \frac{1}{\epsilon_1 2a} \left( \frac{\epsilon_2 - \epsilon_1}{\epsilon_2 + \epsilon_1} \right) q dq = \frac{Q^2}{4\epsilon_1 a} \left[ \frac{\epsilon_1 - \epsilon_2}{\epsilon_1 + \epsilon_2} \right]$$

Note that image charge screening goes as  $Q^2$ !!!

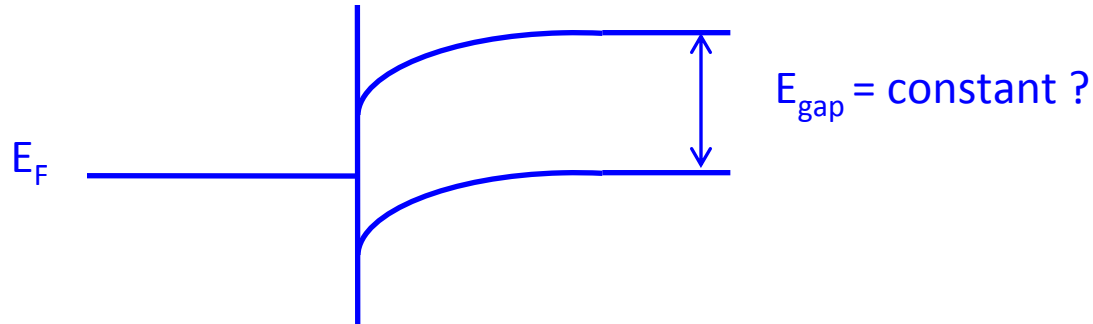
Cannot be treated as a change in single particle potential    ELECTRONIC POLARONS

The energies of electrons (cond. Band ) and holes (valence band) are both lowered

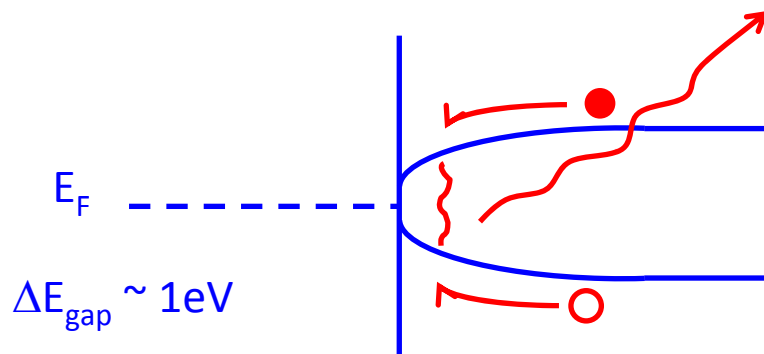
Therefore conductivity gap is lowered

Both electrons and holes will want to move to the interface

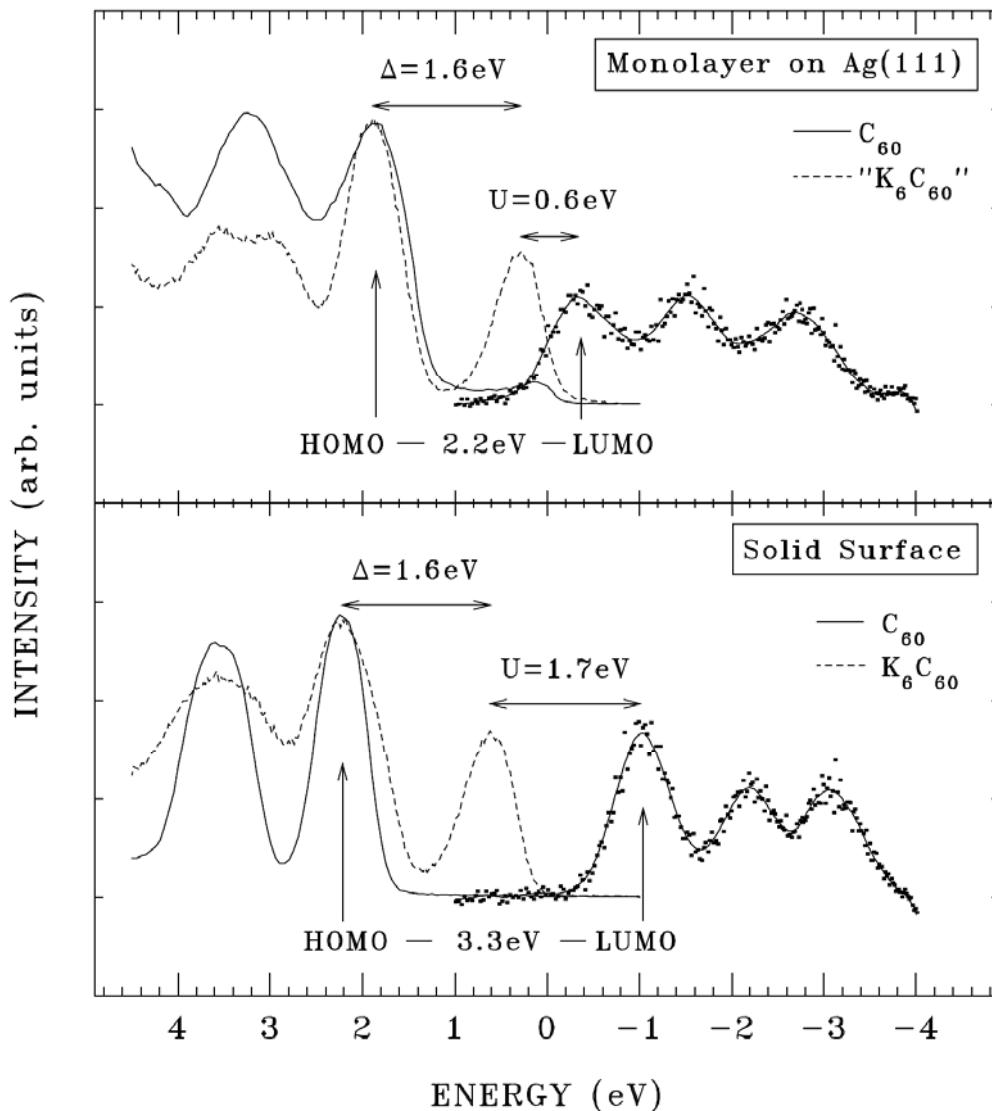
# Conventional wide band semiconductor –metal interface



Narrow band semiconductor –metal interface in which  
The polarization cloud can follow the electron yielding  
“ELECTRONIC POLARON”



Examples are molecular solids , strongly correlated systems , TM, RE-----



Combined photoemission (solid lines) and inverse photoemission (dots with solid lines as guide to the eye) spectra of the  $C_{60}$  monolayer on Ag(111) (upper panel) and the surface layer of solid  $C_{60}$  (lower panel). Also included are the photoemission spectra (dashed lines) of the fully doped  $C_{60}$  (" $K_6C_{60}$ ") monolayer on Ag(111) and the surface layer of solid  $K_6C_{60}$ .

- Band gap is reduced !
- Molecular Orbital Structure is conserved !

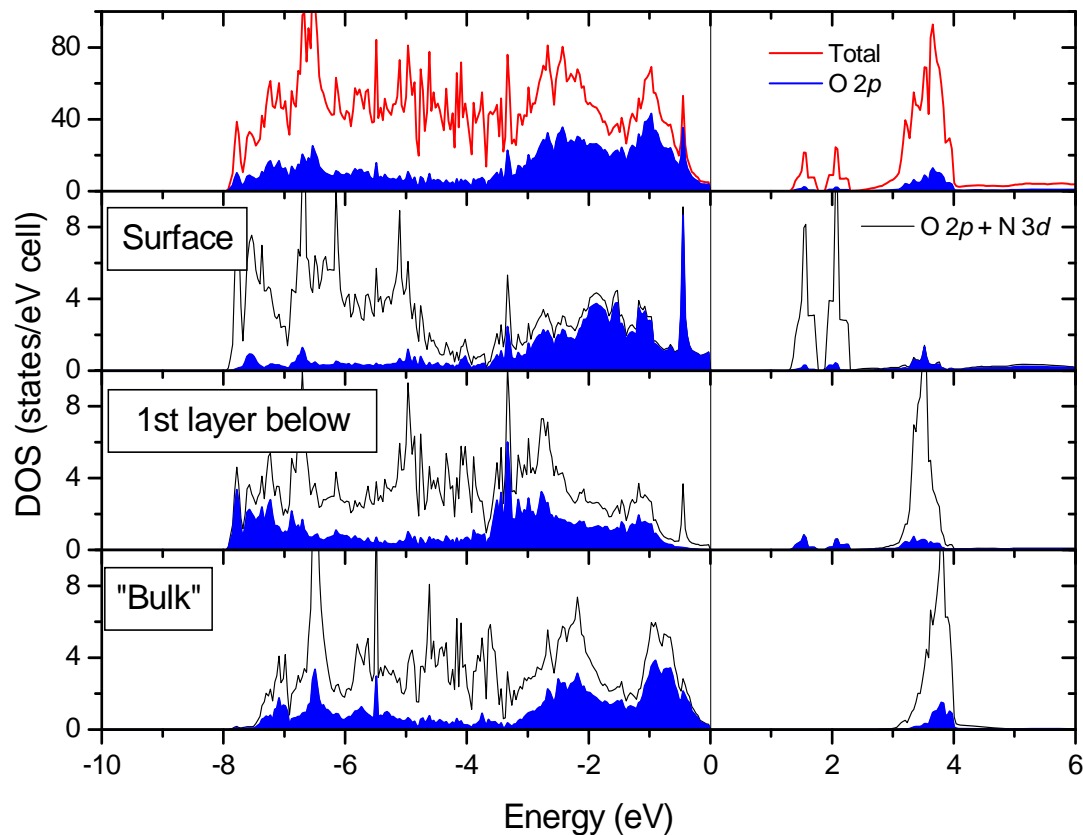
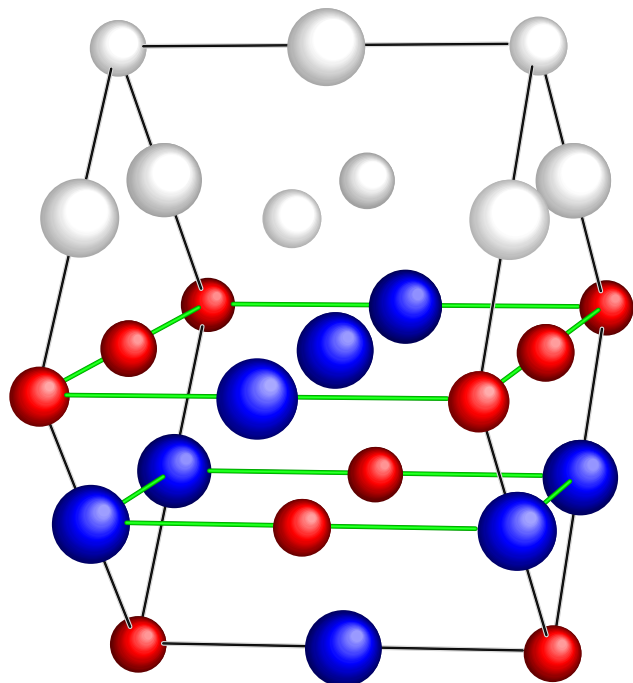
With variable energy PES we could look at this band gap narrowing at the interface Of great importance for molecular electronics, solar cells etc.

# Surfaces and interfaces of narrow band ionic materials

# Neutral (110) surfaces of NiO

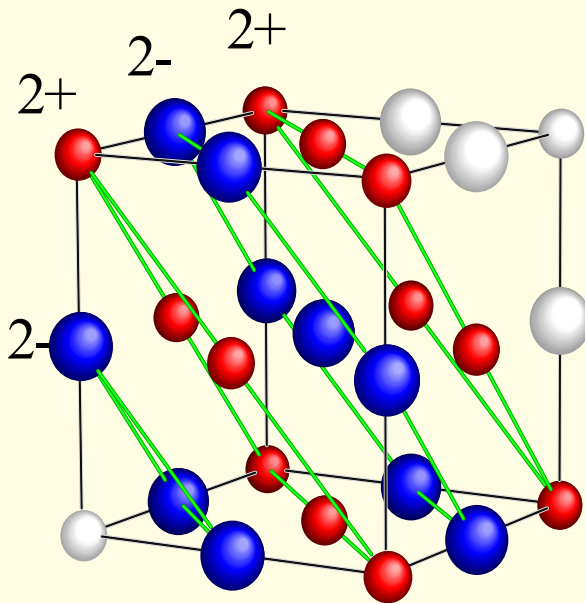
Slab of 7 NiO layers

LSDA+U:  $U=8\text{eV}$   $J=0.9\text{eV}$

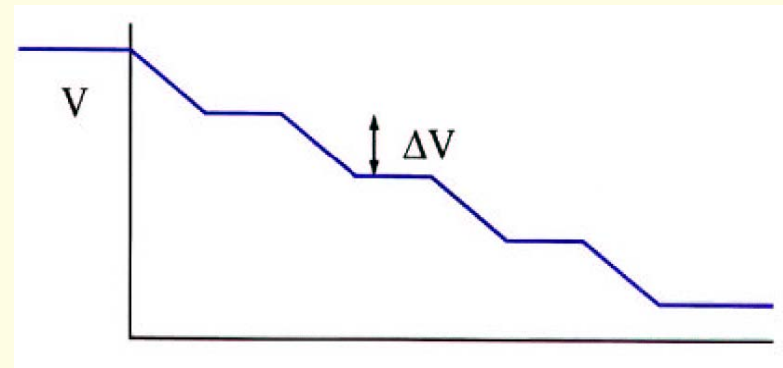
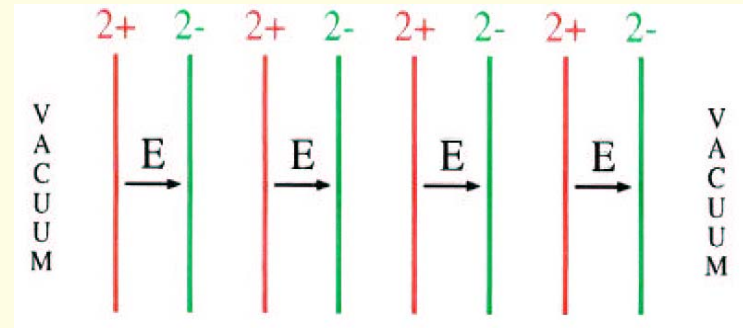


**Band gap at the surface decreases from 3 eV to 1.2 eV**  
**Step edges could be 1D strongly correlated metals**

# Polar (111) Surfaces of MgO



*Finite slab of charged planes*



*$\Delta V=58$  Volt per double layer!*

# Some key papers on polar surfaces and interfaces

R. Lacman, Colloq. Int. C.N.R.S. 152 (1965) 195

D. Wolf, Phys. Rev. Lett. 68 (1992) 3315.

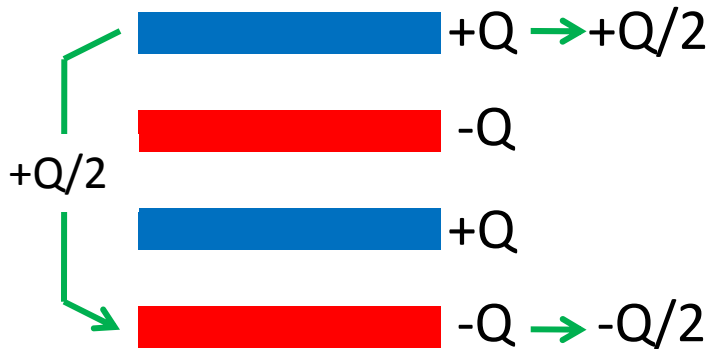
H.-J. Freund and E. Umbach, Eds., Adsorption on Ordered Surfaces of Ionic Solids and Thin Films, Vol. 33 of Springer Series in Surface Science (Springer, Berlin, 1993).

Hesper et al PRB 62, 16046 2000 coined the phrase Electronic Reconstruction for K<sub>3</sub>C<sub>60</sub> surfaces

A. Ohtomo and H. Y. Hwang Nature **427**, 423 (2004)  
Insulating Oxide heterostructures

# Types of reconstruction

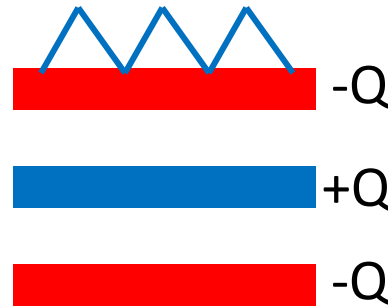
## Electronic



Rearrangement of electrons

$K_3C_{60}$ :  
R. Hesper *et al.*, Phys. Rev. B  
**62**, 16046 (2000).

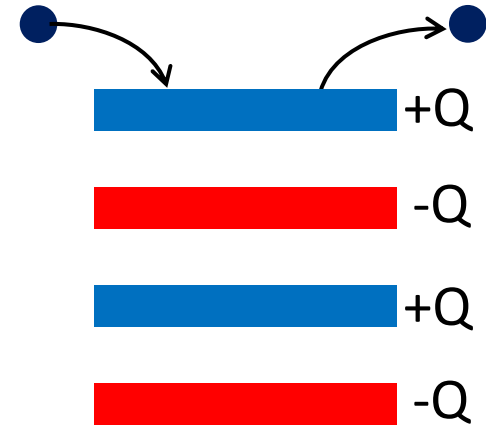
## Ionic



Rearrangement of ions faceting

NiO(111):  
D. Cappus *et al.*, Surf. Sci.  
**337**, 268 (1995).

## Chemical

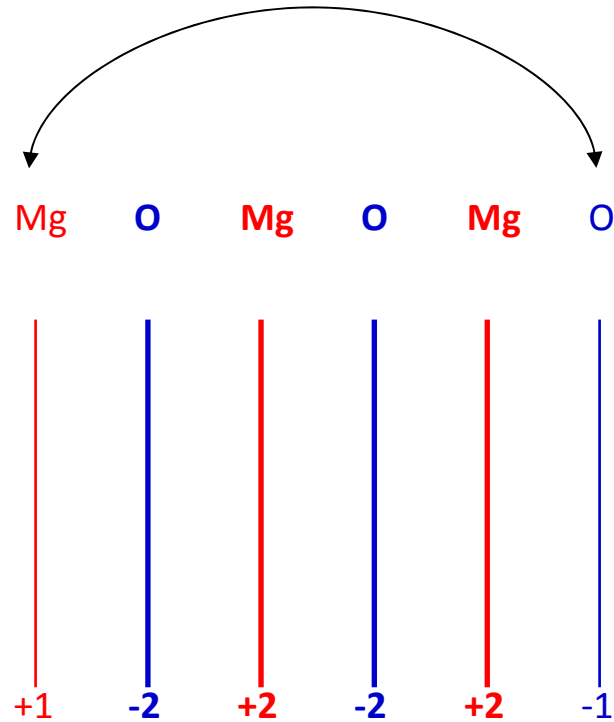


Vacancies or add ions ( $K^+$ ) or  $OH^-$

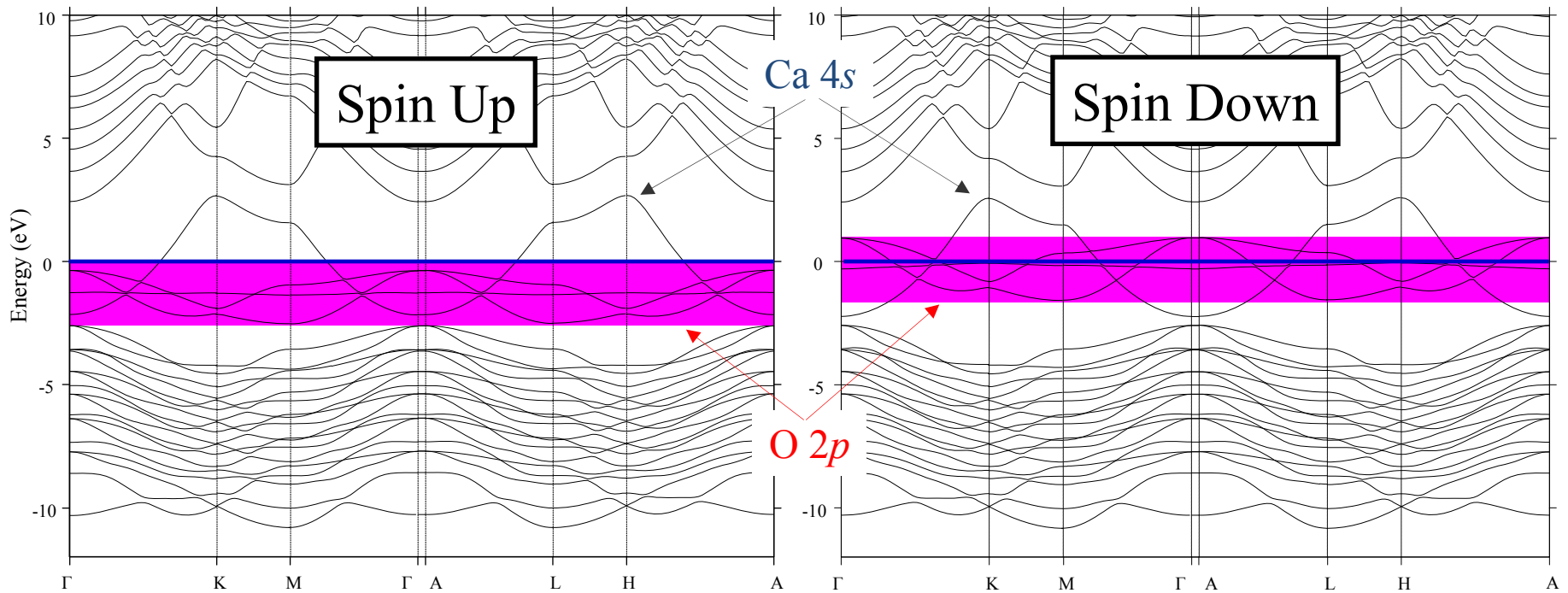
K-depositon:  
M.A. Hossain *et al.*, Nat. Phys.  
**4**, 527 (2008).  
NiO(111):  
D. Cappus *et al.*, Surf. Sci.  
**337**, 268 (1995).

# ELECTRONIC RECONSTRUCTION

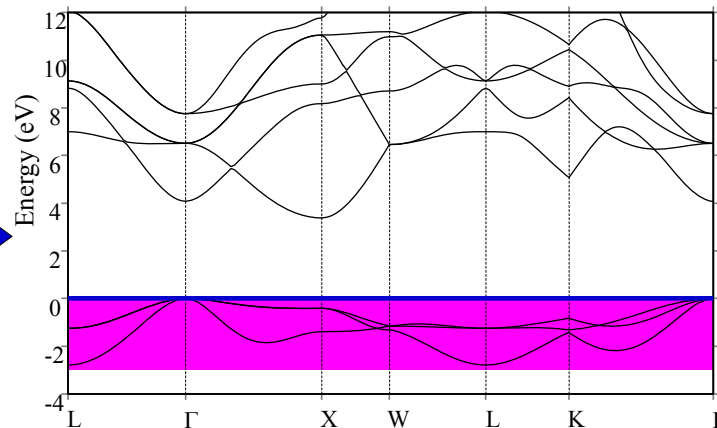
Transfer one electron from O layer to Mg layer



# LSDA Band Structure of CaO (111) Slab terminated with Ca and O



Note:  
Bulk material  
(no surface)  
is an insulator



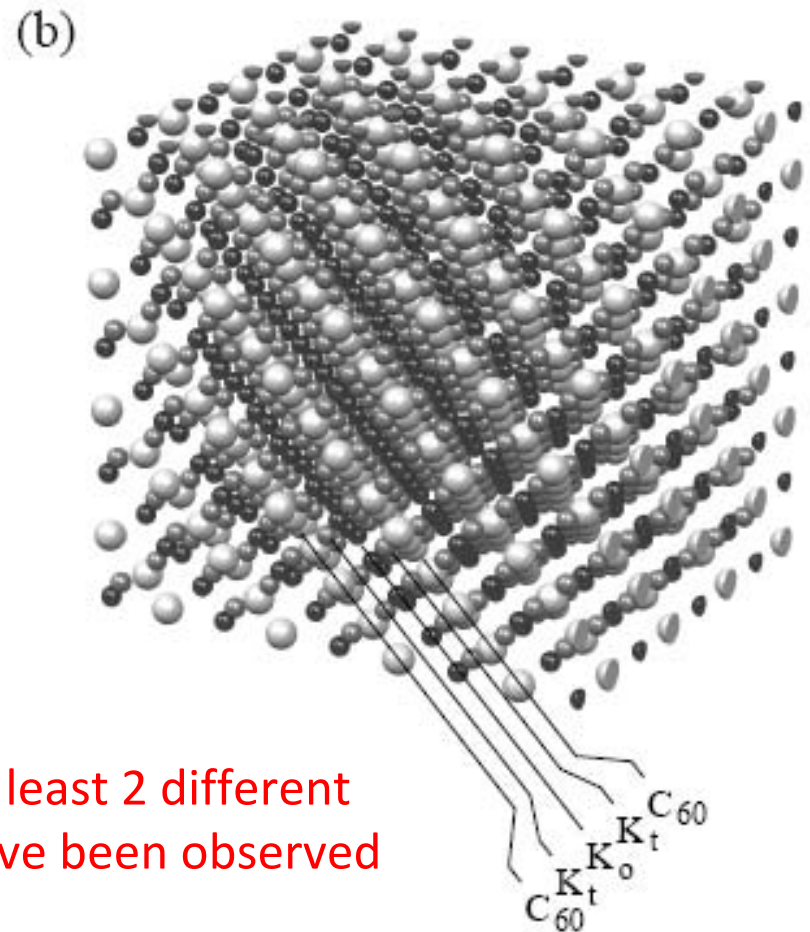
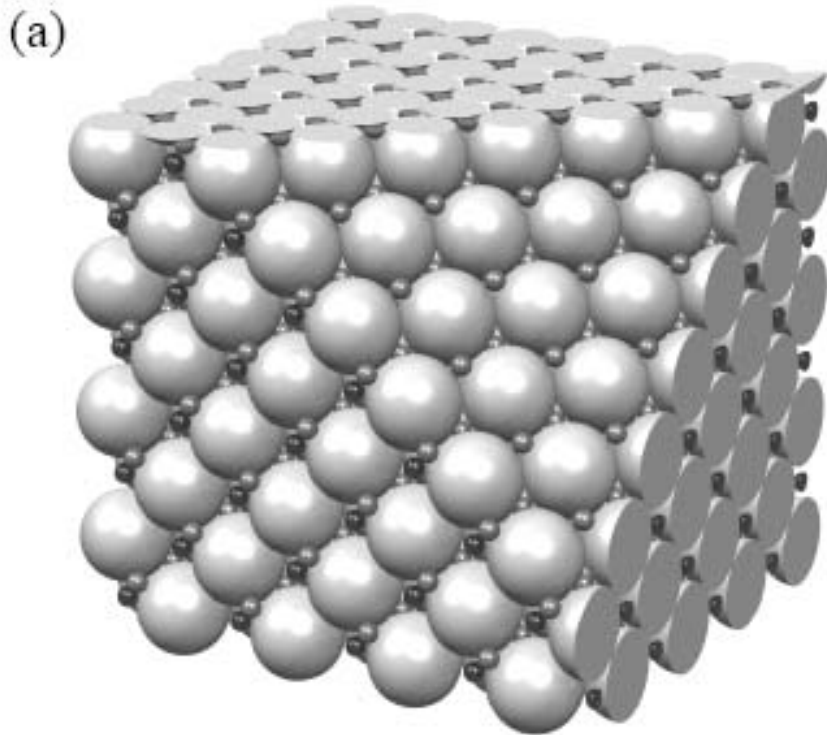
But **surface** is  
**metallic!** And  
**ferromagnetic**

# Electronic Reconstruction

- Energetically favourable in ionic systems with small band gaps and in systems with multivalent components ( Ti, V, C60, Ce, Eu ---- )

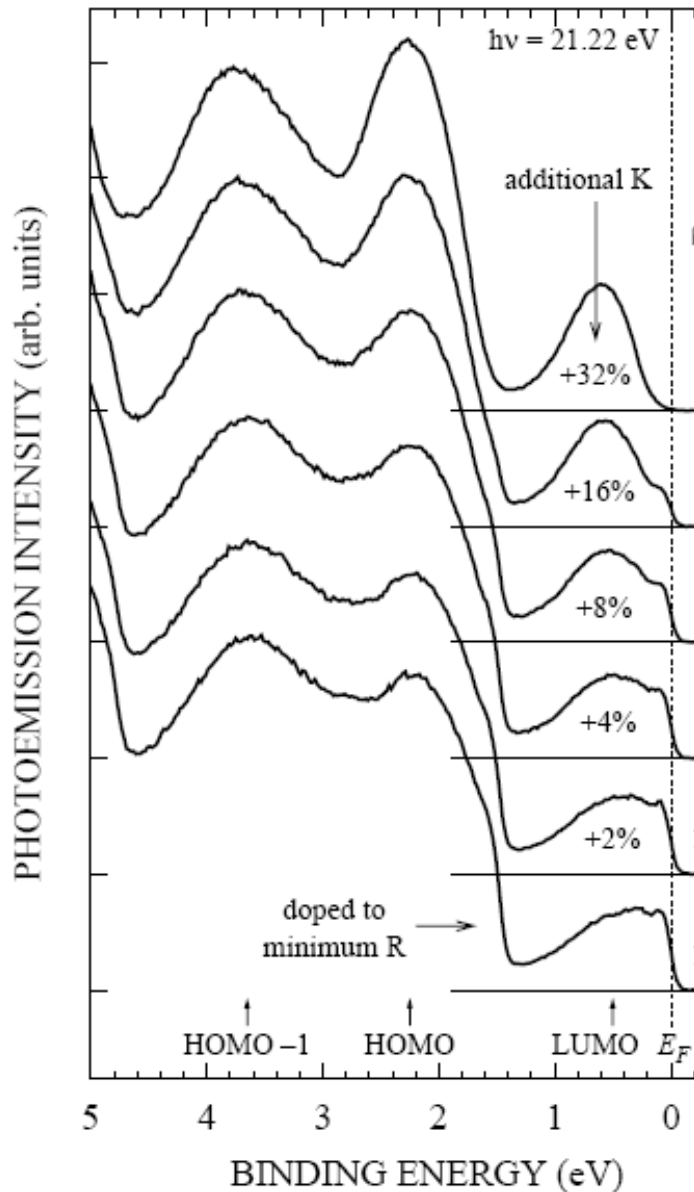
Hesper et al PRB 62, 16046 2000 coined the phrase electronic Reconstruction for K3C60 surfaces

111 surface of K3C60 and its polar nature.



several terminations are possible and at least 2 different Photoemission spectra at the surface have been observed corresponding to C60 1.5-, 2.5-

# Electronic reconstruction of K3C60 surfaces



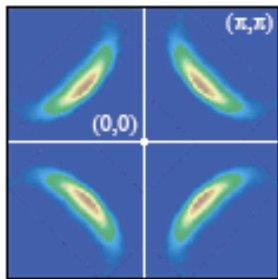
A collection of published Photoelectron spectra of K3C60. The spectra vary from 0.5, 1.5, 2.5 negative charge on C60 depending on the termination

# Examples of ad atom stabilization of Polar surfaces

- NiO grown by MBE is covered by a monolayer of OH<sup>-</sup> = 1/2 the charge of the Ni<sup>2+</sup> layer underneath and therefore stable
- MnS single crystals grown with vapor transport methods yield large crystals with 111 facets???? Covered by a single layer of I<sup>-</sup> and the crystal grows underneath. Like a surfactant
- 1/2 Ba missing on the surface of BaFe<sub>2</sub>As<sub>2</sub>
- Elfimov has DFT calculations of O vacancies , and various forms of add atoms
- K<sup>+</sup> ad ions on YBCO

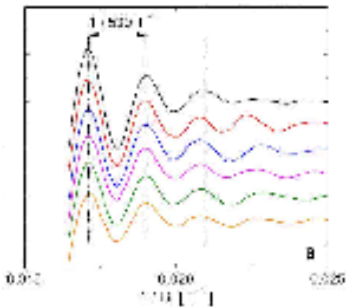
# Fermiology across the Cuprate Phase Diagram

CCOC -  $x=0.12$



ARPES - Shen (05)

YBCO -  $x=0.10$

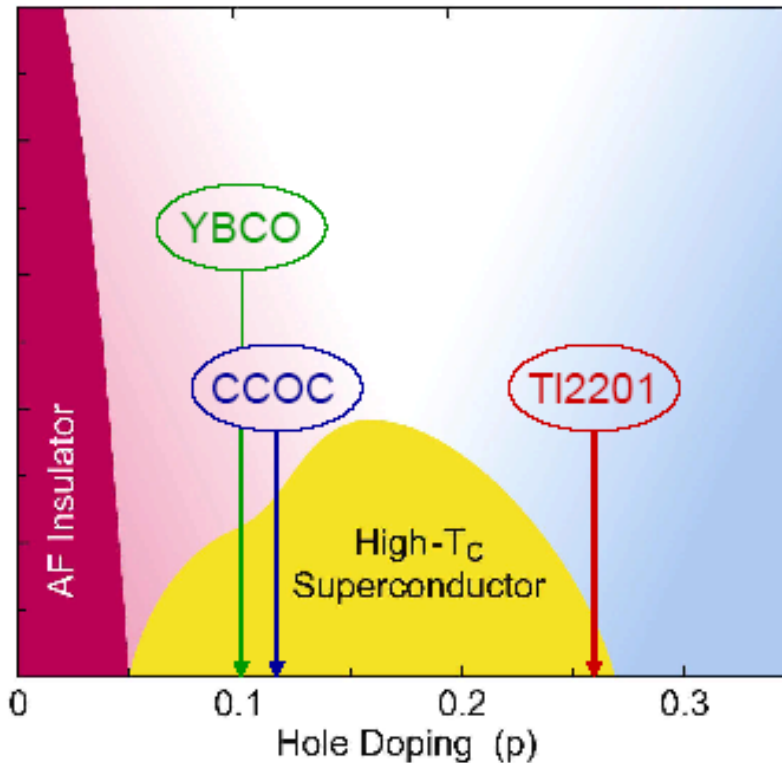


QO - Doiron-Leyraud (07)

ARPES on YBCO6.5

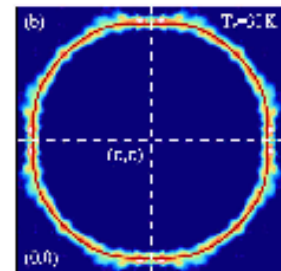
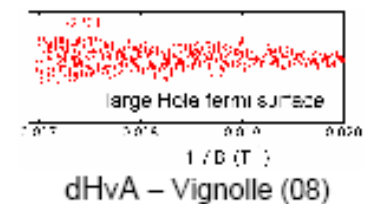
Overdoped Tl2201

Quantitative agreement between single-particle and transport probes

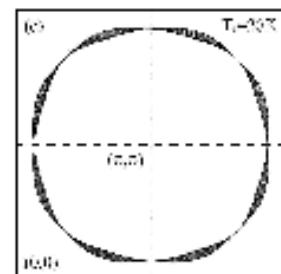


Can this be the gateway to a unified picture for underdoped cuprates?

Tl2201 -  $x=0.26$

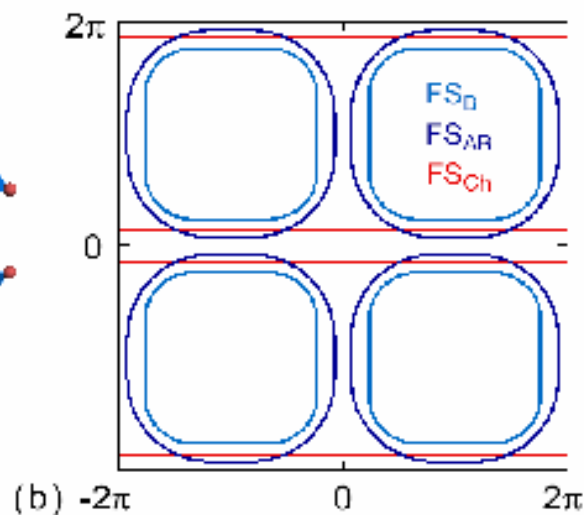
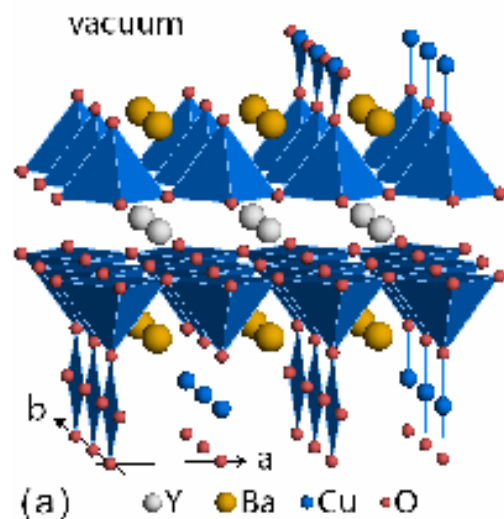


ARPES - Platé (05)

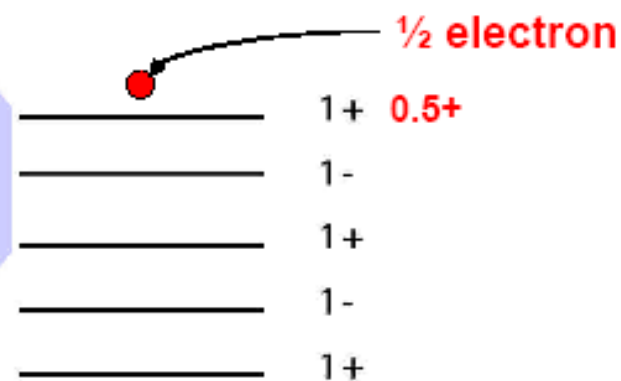


AMRO - Hussey (03)

# Electronic Surface Reconstruction in $\text{YBa}_2\text{Cu}_3\text{O}_{6+x}$



CuO Chain	1+
BaO	0
CuO <sub>2</sub> Plane	2-
Y	3+
CuO <sub>2</sub> Plane	2-
BaO	0
CuO Chain	1+

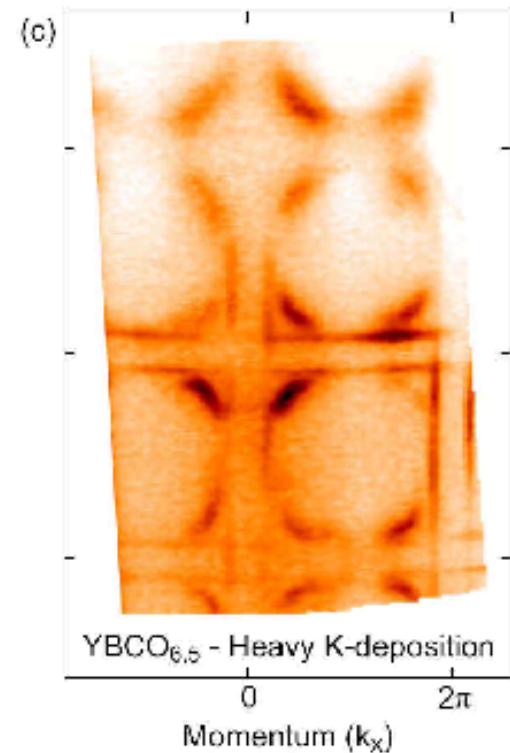
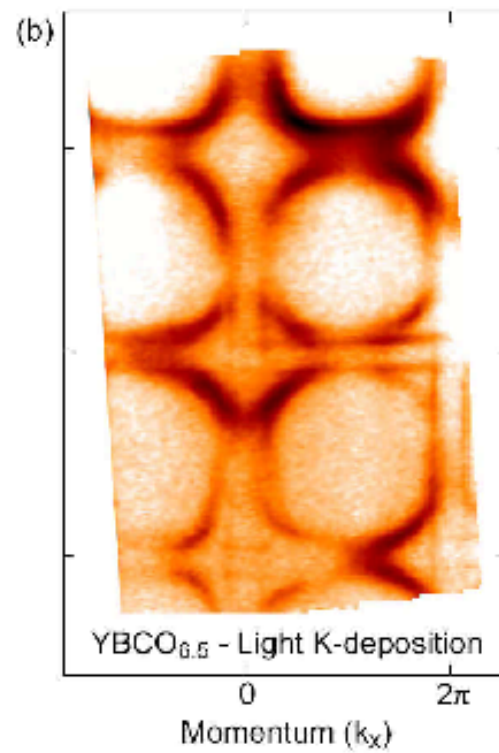
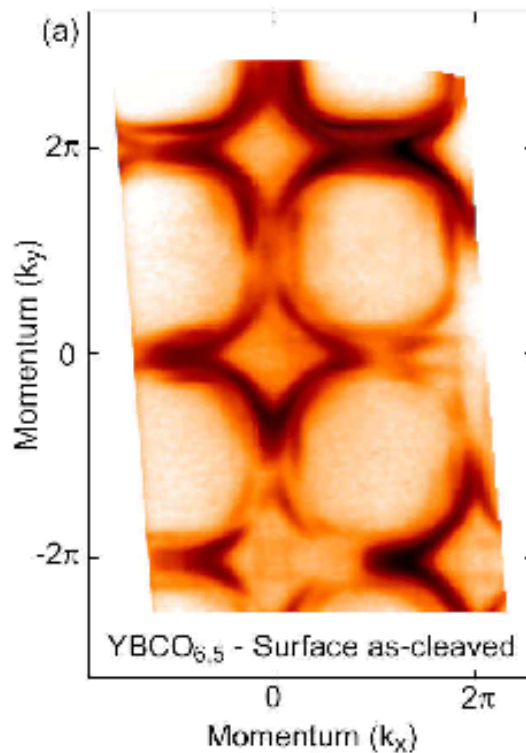


# Our ARPES studies of Ortho-II YBCO<sub>6.5</sub>

**Fresh**

**Surface Treatment 1**

**Surface Treatment 2**



**Electron doping**

**LDA**



**Fermi arcs**

Ilya Elfimov note the potential variation in the slab upon electronic reconstruction. This would cause a systematic core level shift

$(\text{YAlO}_3)_{16}$  slab

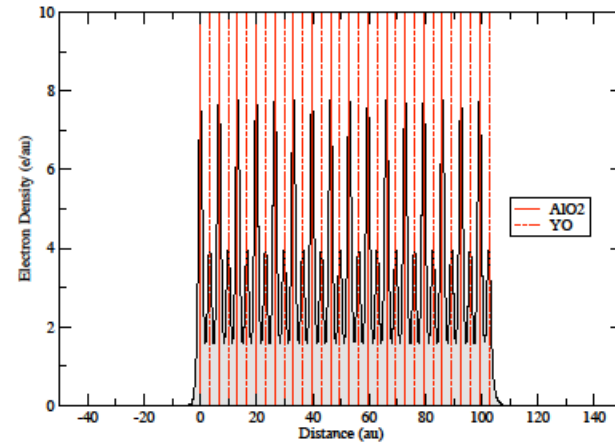
The same potential drop as in a case of 5 unit cells

$$\Delta V = \text{const}$$

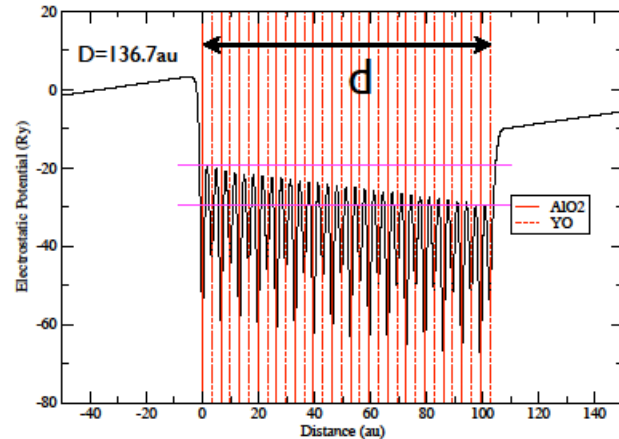


$$E \sim \frac{1}{d}$$

Very strange!



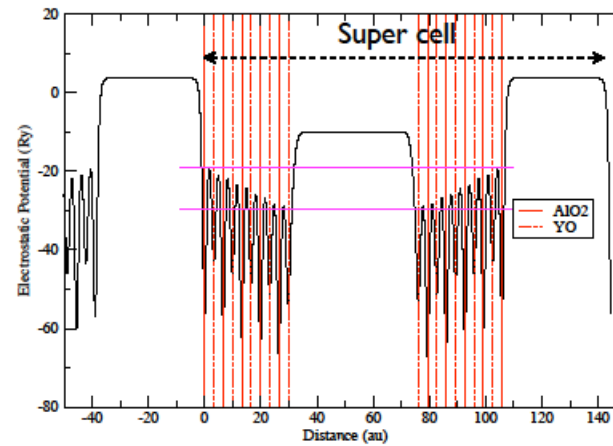
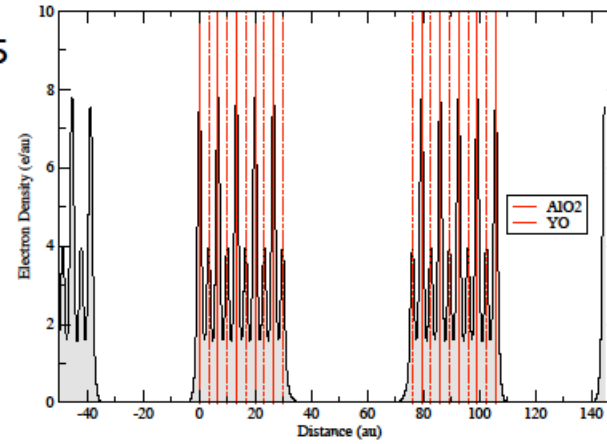
Bulk potential



Slab with electronic reconstr.

$(\text{YAIO}_3)_5$  -- vacuum --  $(\text{YAIO}_3)_5$   
slab

YAIO slabs arranged in reverse



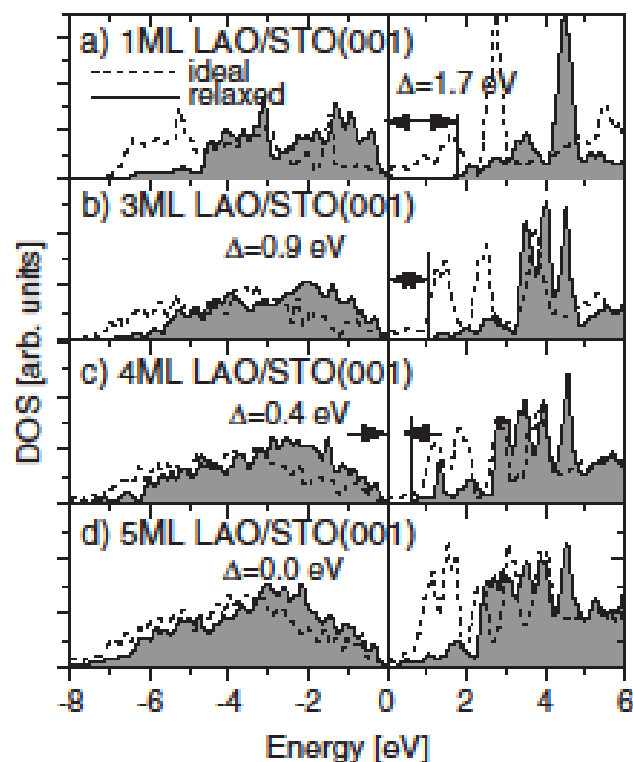


FIG. 3. Density of states for the ideal (dashed line) and relaxed (solid line, grey filling) structure of 1–5 ML LAO on STO(001). Relaxation opens a band gap, but its size decreases with each added LAO layer.

$\epsilon = 24$ , this becomes approximately  $\Delta V = 4\pi e \frac{D_{\text{relax}}}{e(3.9 \text{ \AA})^2} \sim 3.5 \text{ eV}$ , which can be sustained by the 5.6 eV gap of LAO.

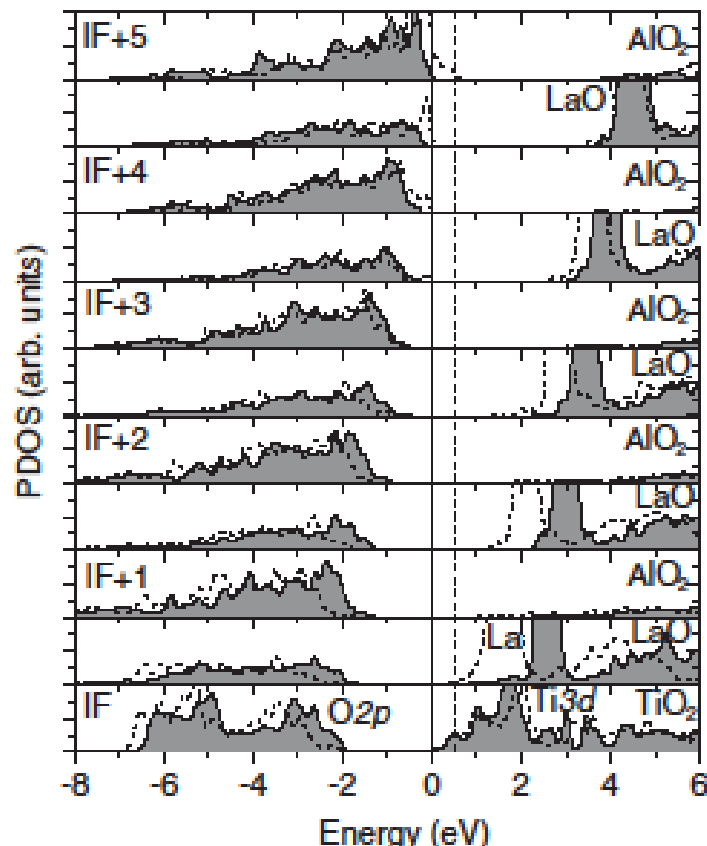


FIG. 4. Layer-resolved density of states of 5 ML LAO on STO(001) with ideal (dashed line) and relaxed (grey shaded area) coordinates. The DOS for the ideal positions was shifted by 0.5 eV to align with the conduction band of the system with the relaxed atomic positions. Its Fermi level is marked with a dashed line.

# Atomic reconstruction

Facetting or ion displacements forming dipole moments to compensate for the electric field.

Pentcheva and Pickett

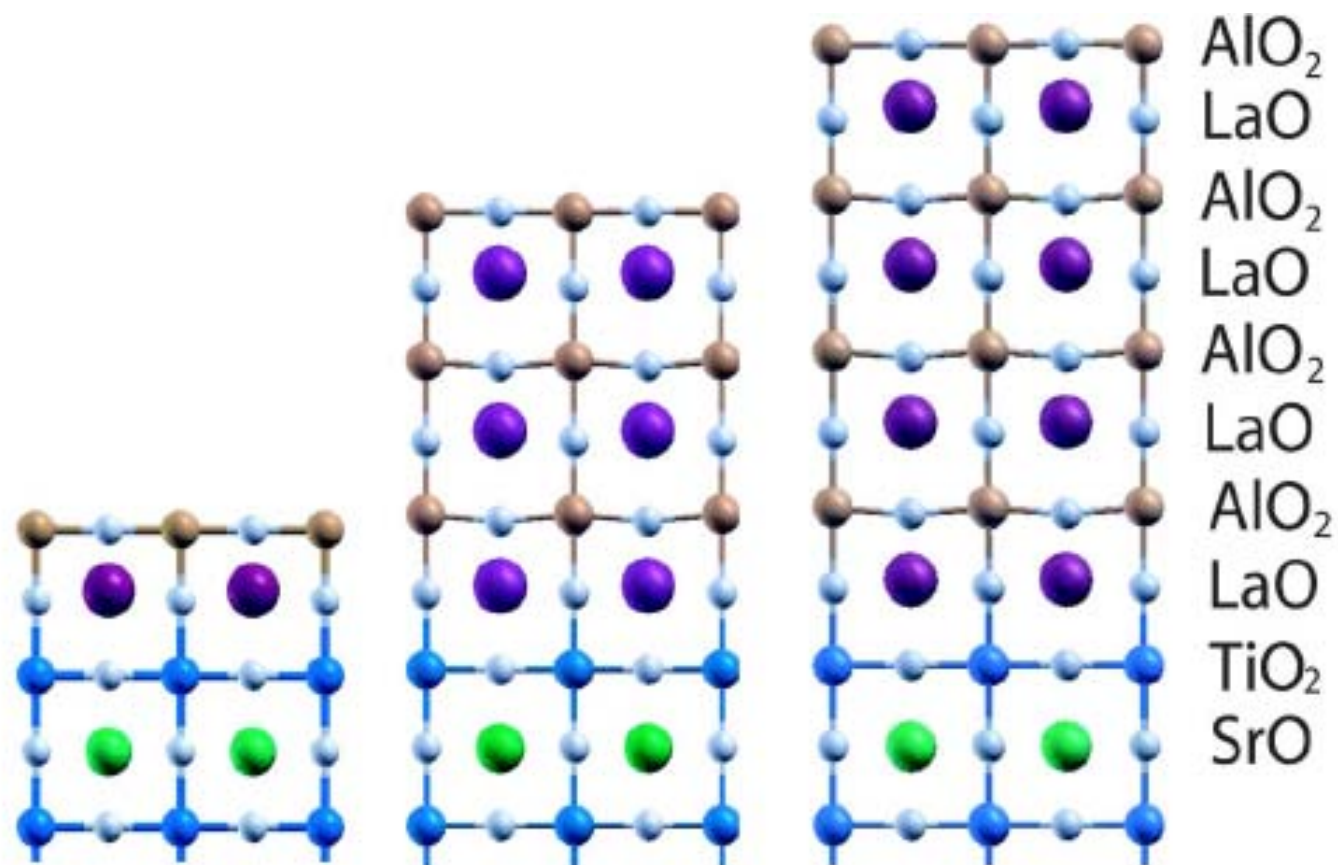


FIG. 1 (color online). Side view of the relaxed structures of 1, 3, and 4 ML LAO on STO(001) showing the polar distortion. The oxygen ions are marked by light grey spheres, while the Sr-, La-, Ti-, and Al-cations are shown by large green (grey), purple (dark grey) and small blue (dark grey) and orange (grey) spheres.

## Avoiding the Polarization Catastrophe in LaAlO<sub>3</sub> Overlayers on SrTiO<sub>3</sub>(001) through Polar Distortion

Rossitza Pentcheva<sup>1</sup> and Warren E. Pickett<sup>2</sup>

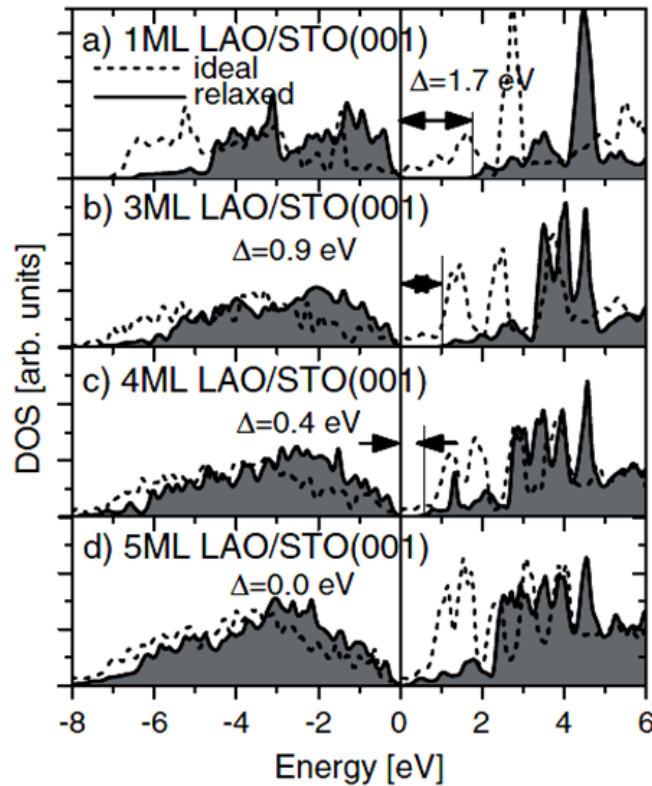


FIG. 3. Density of states for the ideal (dashed line) and relaxed (solid line, grey filling) structure of 1–5 ML LAO on STO(001). Relaxation opens a band gap, but its size decreases with each added LAO layer.

$\epsilon = 24$ , this becomes approximately  $\Delta V = 4\pi e \frac{D_{\text{dipole}}}{\epsilon(3.9 \text{ \AA})^2} \sim 3.5 \text{ eV}$ , which can be sustained by the 5.6 eV gap of LAO.

The dipole shift due to the polar distortion can be

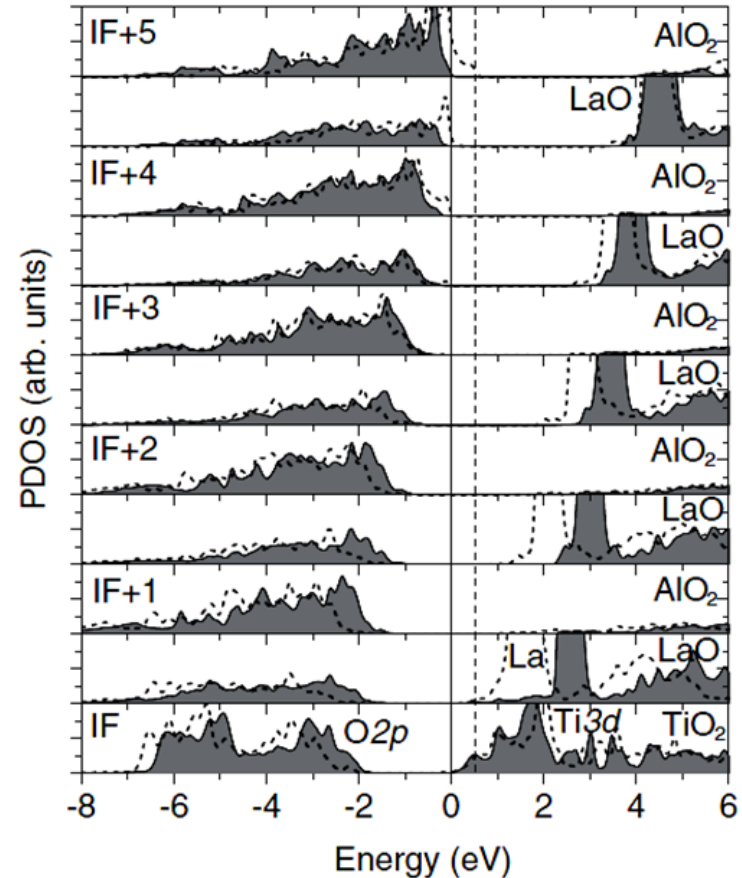


FIG. 4. Layer-resolved density of states of 5 ML LAO on STO(001) with ideal (dashed line) and relaxed (grey shaded area) coordinates. The DOS for the ideal positions was shifted by 0.5 eV to align with the conduction band of the system with the relaxed atomic positions. Its Fermi level is marked with a dashed line.

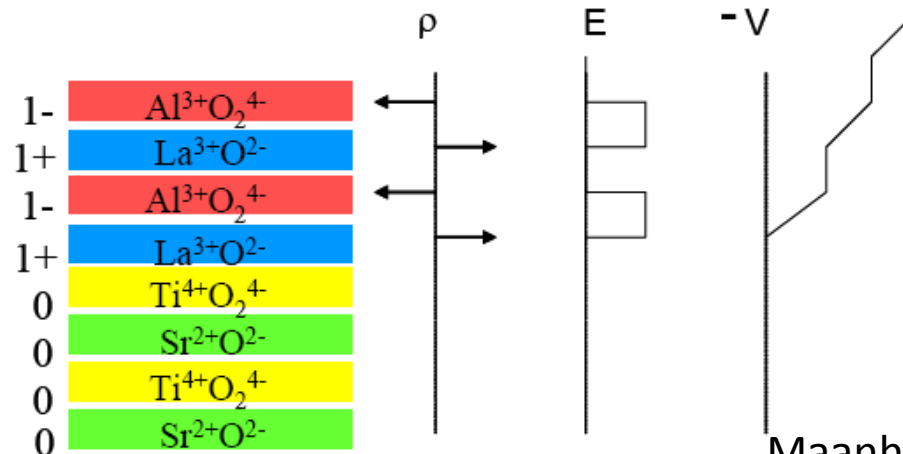
# Interfaces involving polar surfaces

Interfaces between polar and non polar surfaces as  
In SrTiO<sub>3</sub> and LaAlO<sub>3</sub> for example can be magnetic  
And Metallic . They will be “self doped” perhaps even  
superconducting

The best candidates for electronic reconstruction  
at surfaces and interfaces is if one component does  
not mind changing its valence !

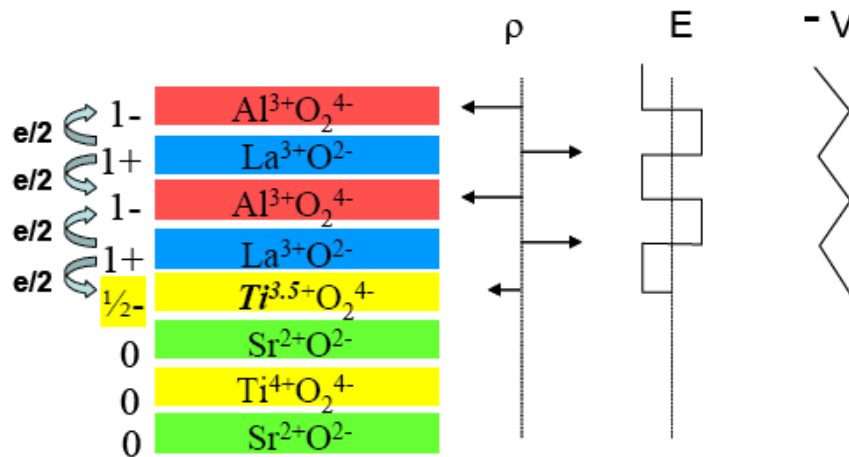
So use systems exhibiting multi valence or mixed  
valence behaviour Ti,V, are good examples

A. Ohtomo, and H.Y. Hwang, *Nature* **427**, 423 (2004).



Maanhart et al MRS buletin review

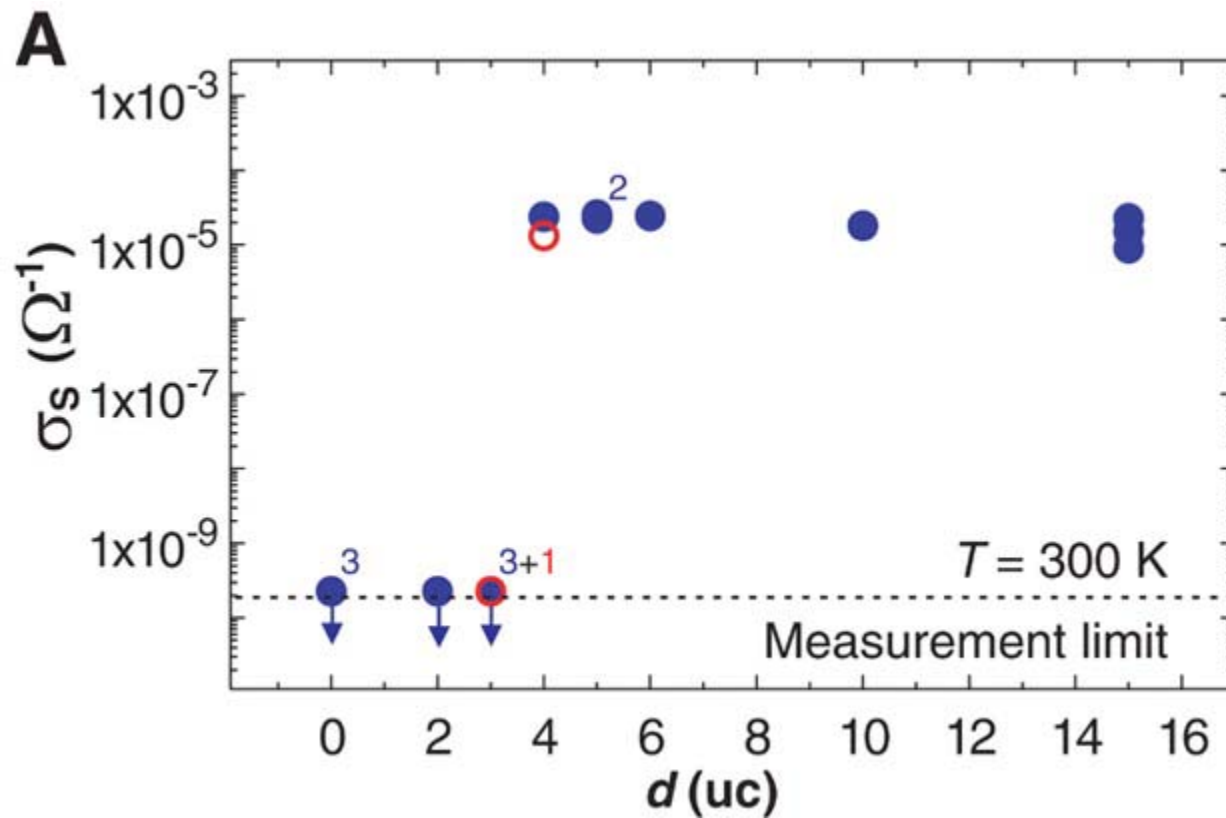
*Resp*



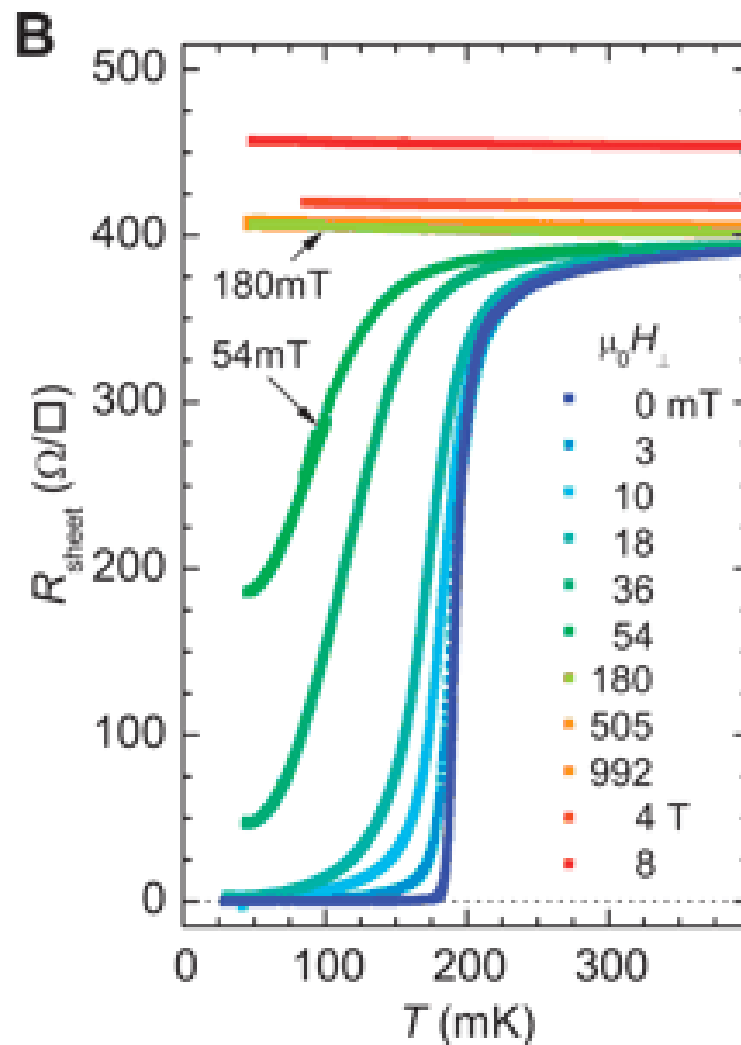
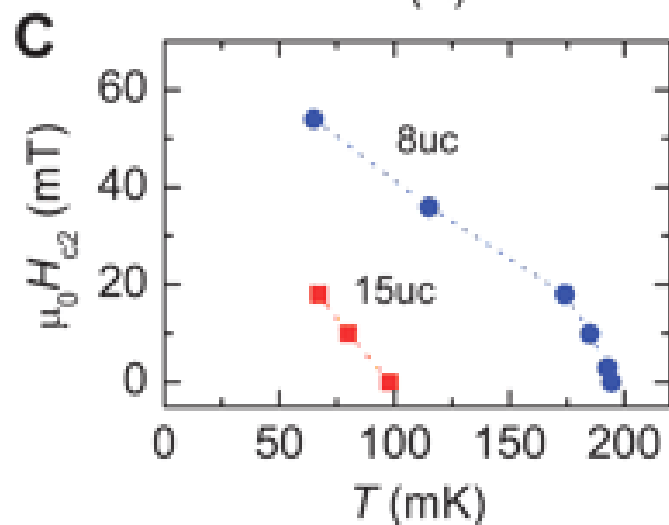
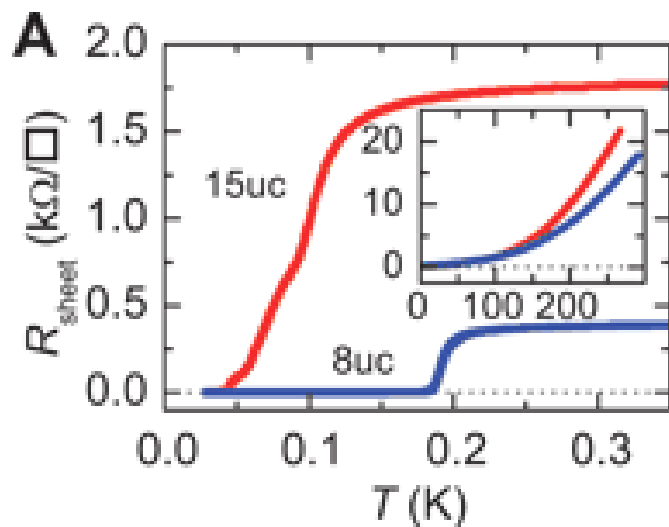
**electronic reconstruction –  
metallic interface**

S.Thiel et al Science 313, 1942 (2006)

Influence of the La AlO<sub>3</sub> thickness on a SrTiO<sub>3</sub> substrate on the conductivity



## Superconducting interface SrTiO3/LaAlO3



These are all great problems for photoelectron spectroscopies and especially high energy PES .

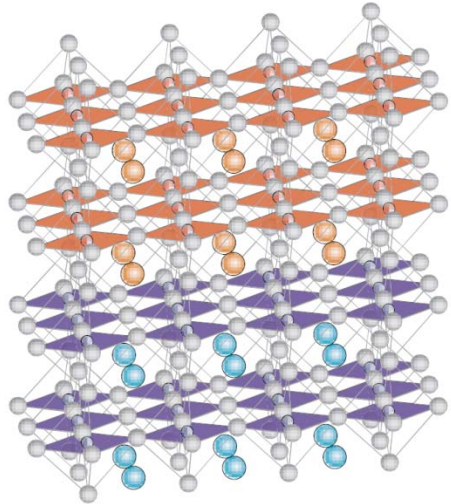
However there is competition with x ray scattering methods like resonant elastic x ray scattering

HOWEVER X ray absorption and scattering involve charge conserving excitations and so cannot identify a Fermi level

This is a big advantage of PES

# Interfaces between transition-metal oxides

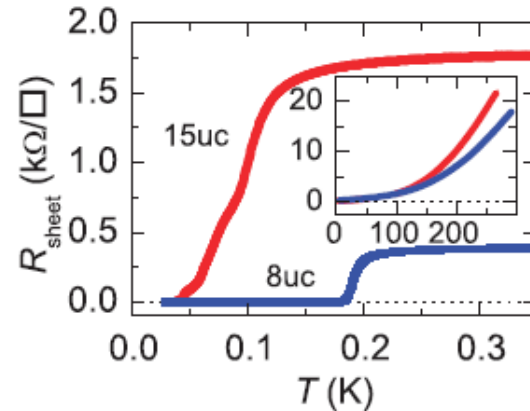
## SrTiO<sub>3</sub>/LaAlO<sub>3</sub> interface



(AlO<sub>2</sub>)<sup>-</sup>  
 (LaO)<sup>+</sup>  
 (AlO<sub>2</sub>)<sup>-</sup>  
 (LaO)<sup>+</sup>  
 (TiO<sub>2</sub>)<sup>0</sup>  
 (SrO)<sup>0</sup>  
 (TiO<sub>2</sub>)<sup>0</sup>  
 (SrO)<sup>0</sup>

Two band insulators  
 LaAlO<sub>3</sub>  
 (Band gap: 5.6 eV)  
 SrTiO<sub>3</sub>  
 (Band gap: 3.2 eV)

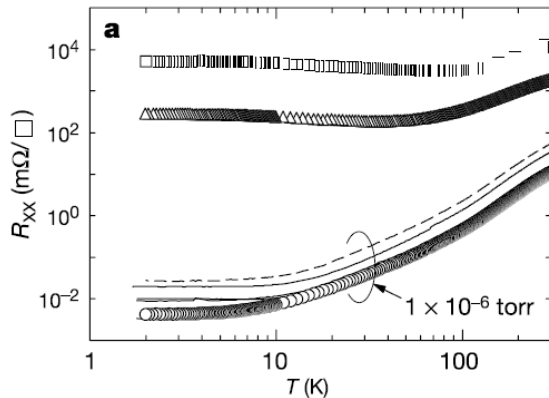
## Superconductivity



$T_c \sim 200$  mK  
 N. Reyren *et al.*,  
 Science **317**,  
 1196 (2007).

## Metallic conductivity

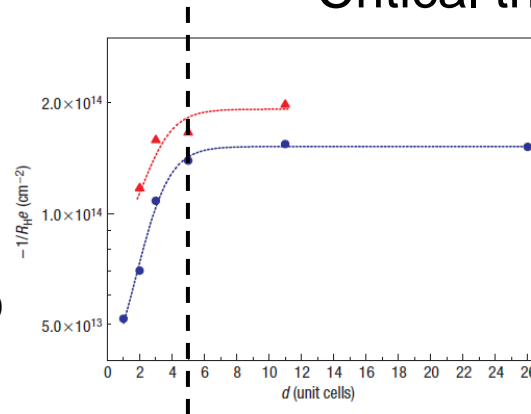
LaAlO<sub>3</sub> (60 Å) / SrTiO<sub>3</sub>(001)



Only *n*-type  
 (LaO)<sup>+</sup>/(TiO<sub>2</sub>)<sup>0</sup>  
 interface is  
 metallic.

A. Ohtomo and H. Y. Hwang,  
 Nature **427**, 423 (2004).

## Critical thickness



Critical thickness  
 of about 5 uc.  
 (Insulating or  
 metallic.)

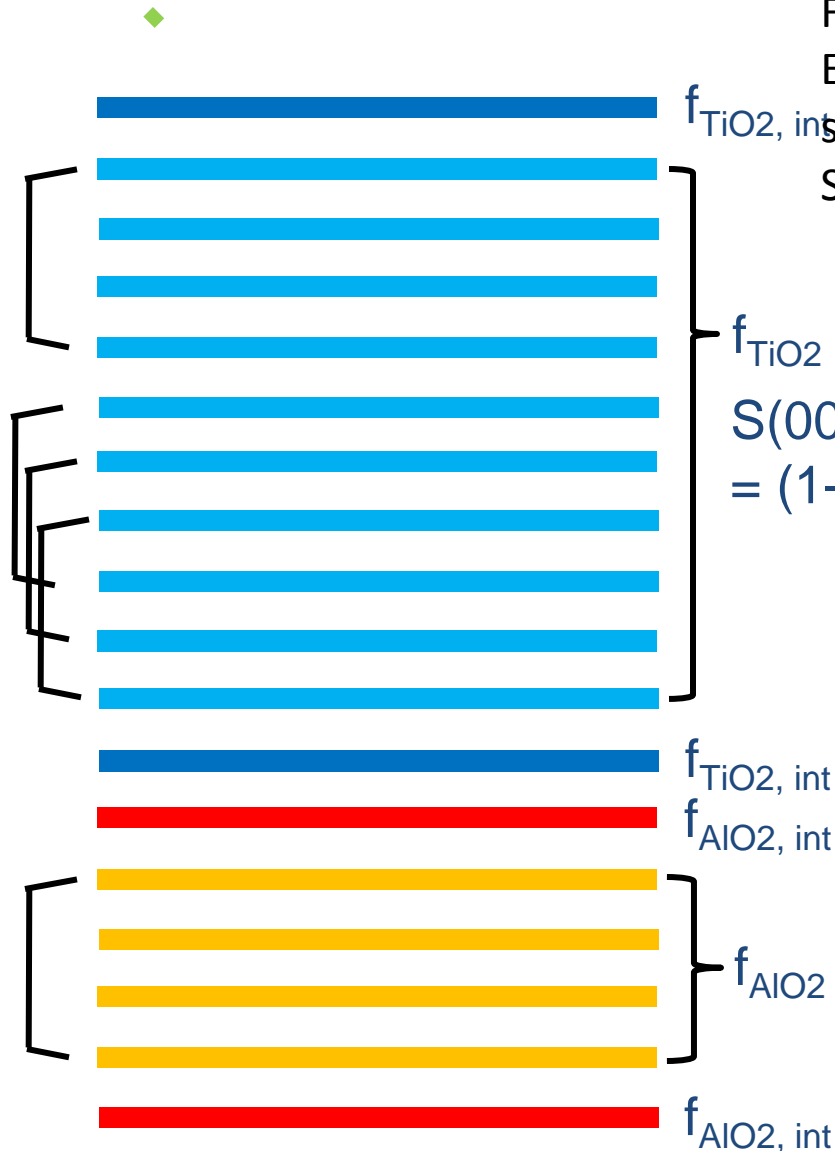
M. Huijben *et al.*, Nat.  
 Mater. **5**, 556 (2006).



What is the electronic structure at the  
 interface? (Electronic reconstruction  
 or oxygen vacancies?)

# Structure factors

Following the ideas presented in  
 Electronic reconstruction at SrMnO<sub>3</sub> – LaMnO<sub>3</sub>  
 superlattice interfaces PRL **99**, 196404 (2007)  
 Serban Smadici, Peter Abbamonte et al



$S(003)$

$$= (1 - \exp(-2\pi i/3))(f_{\text{TiO}_2, \text{int}} - f_{\text{TiO}_2} + f_{\text{AlO}_2, \text{int}} - f_{\text{AlO}_2})$$

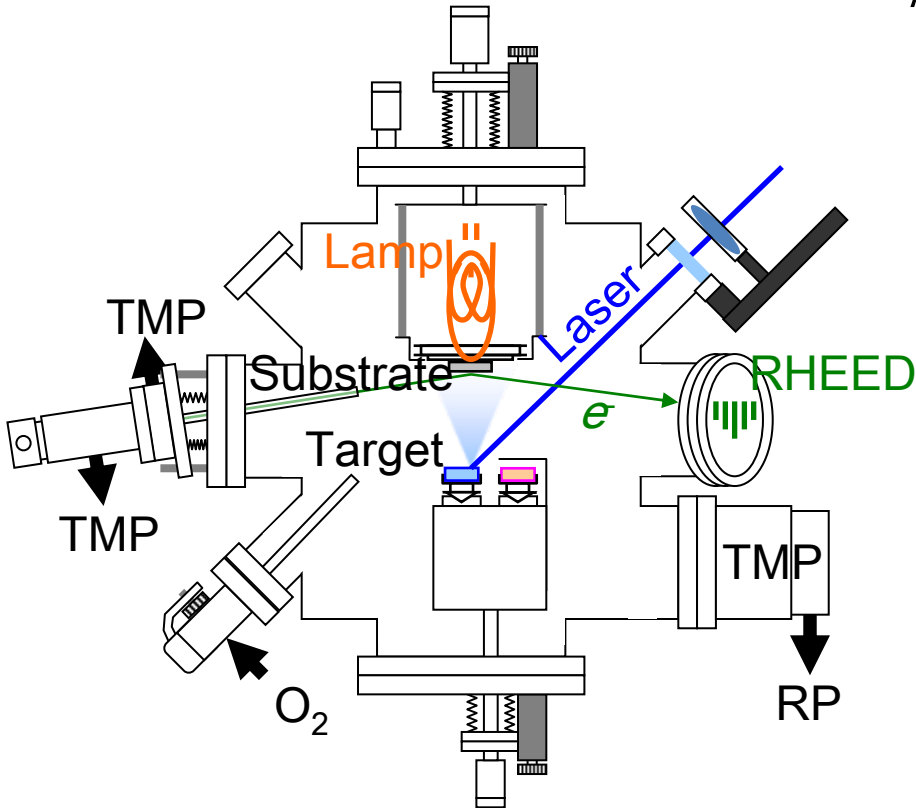
If  $f_{\text{TiO}_2, \text{int}} = f_{\text{TiO}_2}$  and  $f_{\text{AlO}_2, \text{int}} = f_{\text{AlO}_2}$   
 (no electronic reconstruction),  
 (003) is forbidden.

➔ (003) is sensitive to the  
 electronic structures at the  
 interfaces.

# Experiment

- Growth technique

Pulsed Laser Deposition (PLD)



Laser: KrF excimer laser ( $\lambda = 248$  nm)

- Sample

$[(\text{SrTiO}_3)_{12}/(\text{LaAlO}_3)_6]_{\text{SL}} * 7$   
/ $\text{SrTiO}_3(001)$

Growth conditions

$P_{\text{O}_2} : 1.0 \times 10^{-5}$  Torr

$T_{\text{sub}} : 800$  °C

Laser : fluency 2 J/cm<sup>2</sup>,  
spot size 2.0 mm<sup>2</sup>

- Soft x-ray scattering measurements

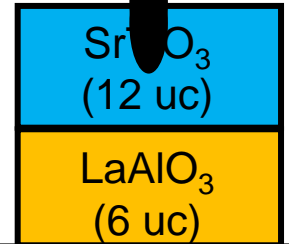
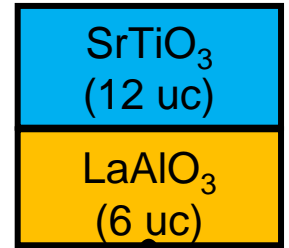
BESSY II UE46 (Berlin, Germany)

NSRRC EPU BL 5 (Hsinchu, Taiwan)

Measurement conditions

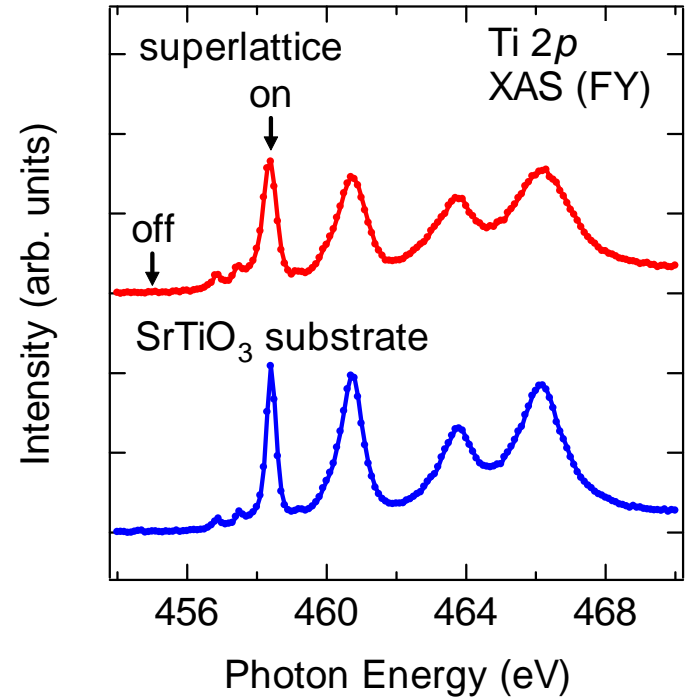
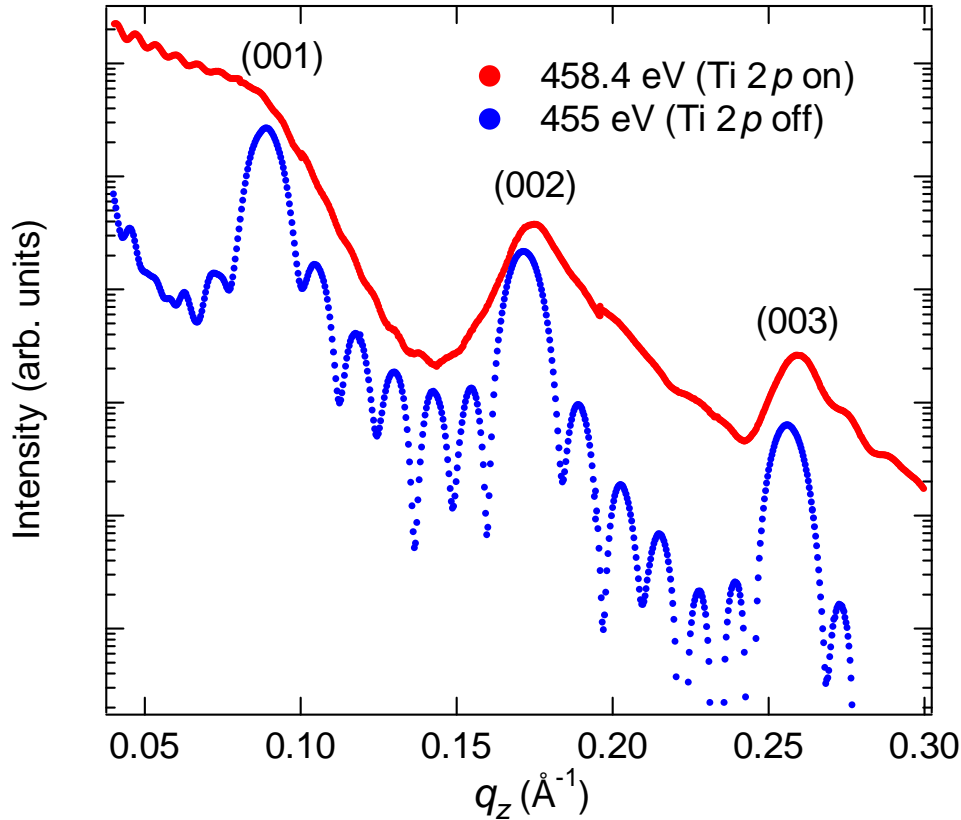
$P \sim 10^{-8}$  Torr,  $T = 80$  K, R.T.

$\sigma, \pi$ -polarization



$\text{SrTiO}_3(001)$

# Reflectivity



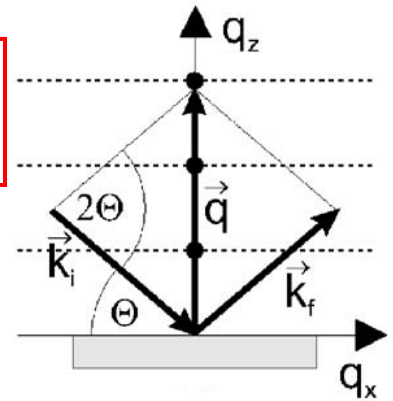
Ti is almost 4+ in the SL.

Oscillations due to 7 periods of superlattice structures.

(003) peak is observed even at off-resonance.

$T = 80$  K,  $\pi$ -polarization

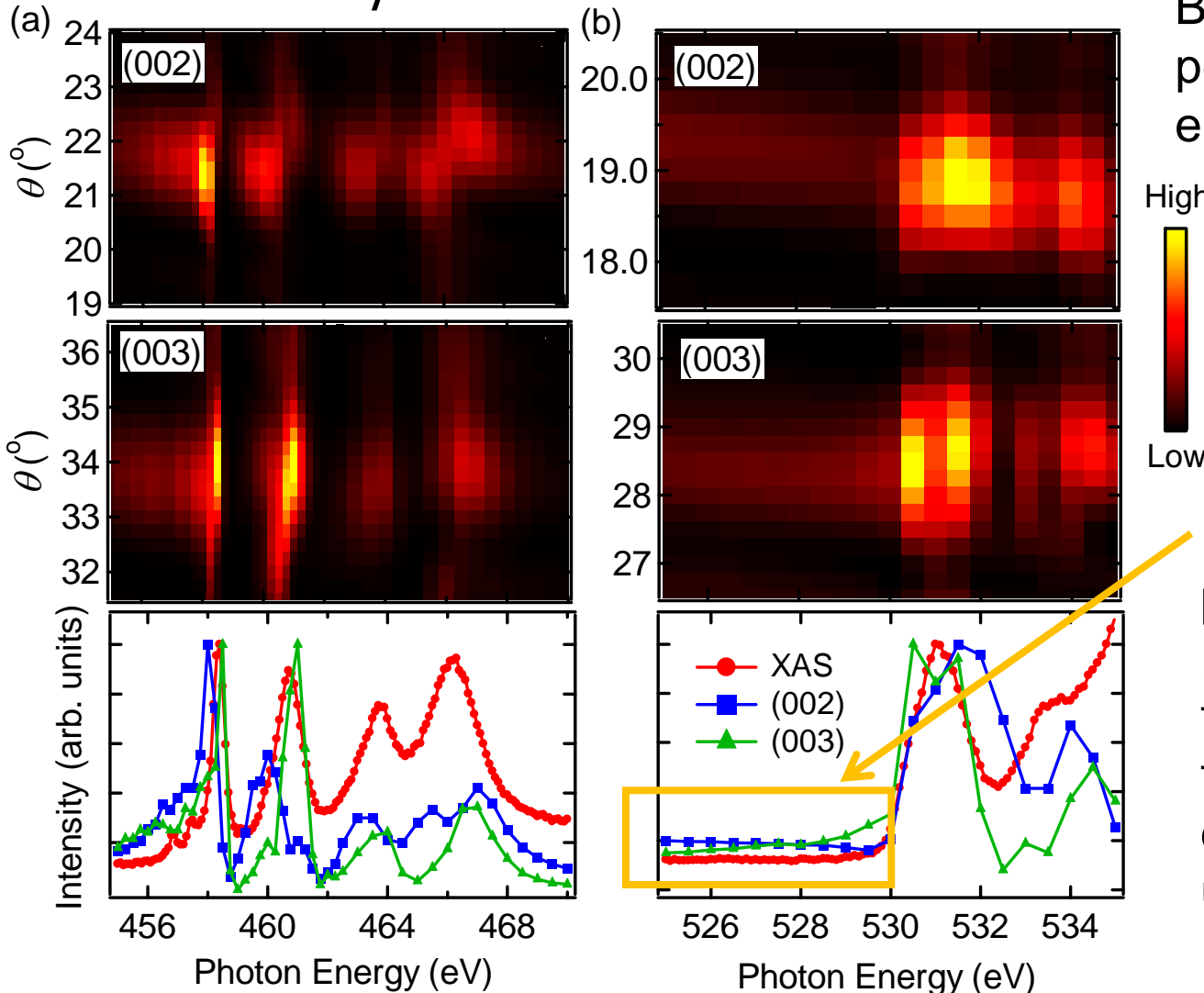
Specular reflection



# Photon-energy dependence

Ti 2p

O 1s



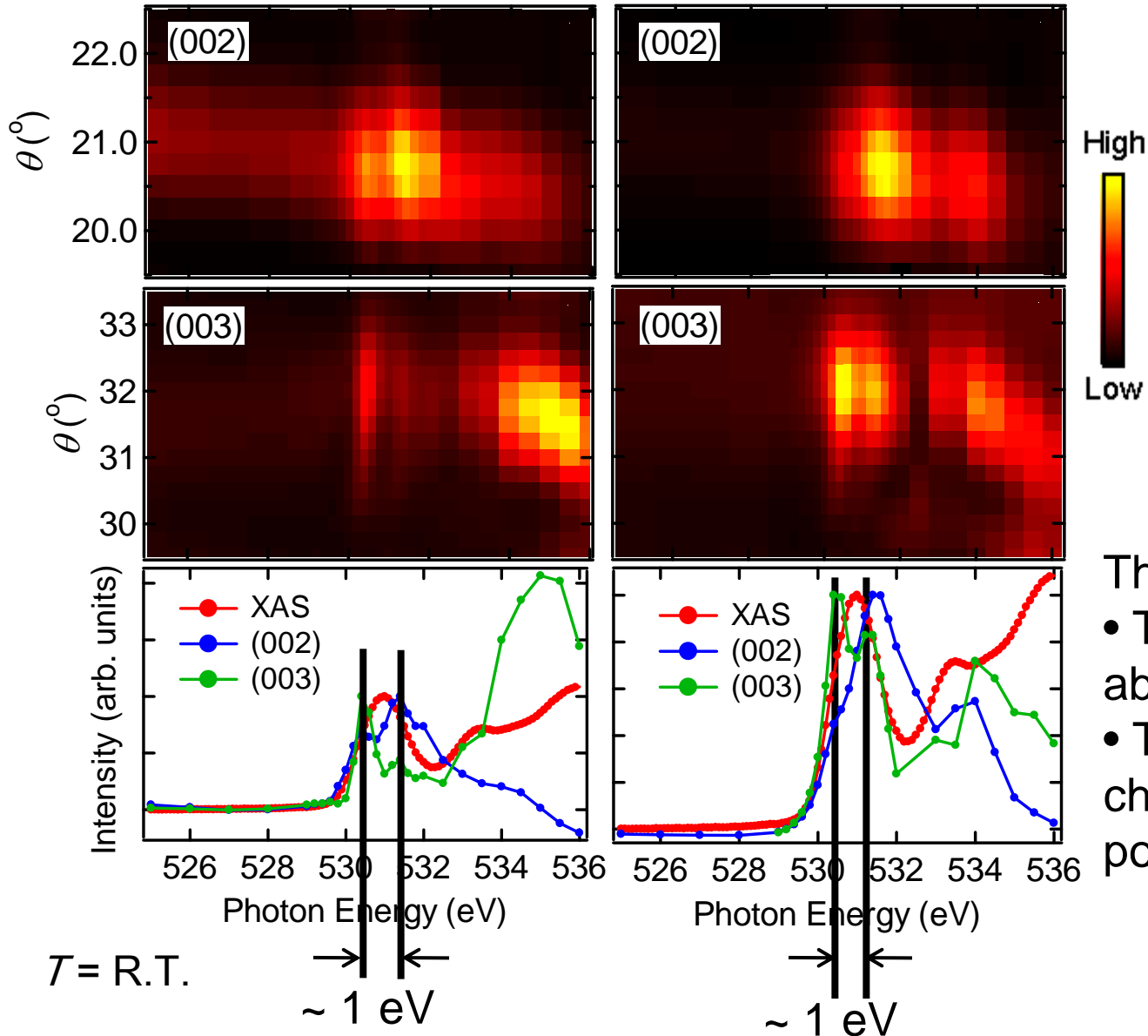
Both the (002) and (003) peaks show resonant enhancement.

In O 1s, there are no pre-edge structures. Metallic behavior due to electron doping to insulating SrTiO<sub>3</sub> does not create new unoccupied states.

# Polarization dependence at O 1s edge

$\sigma$ - polarization

$\pi$ - polarization



Strong polarization dependence!

There are two structures.

- The energy splitting is about 1 eV.
- The relative intensities change by changing polarization.

# Conclusions

- We need all of the techniques mentioned .
- Each has its advantages and disadvantages
- Hard x ray photoemission will, become especially important if the energy and momentum resolution can be improved.
- To study buried interfaces we will need a suite of methods including also the TEM based EELS with good spatial and spectroscopic energy resolution

For narrow band materials like molecular solids, strongly correlated transition metal compounds etc the induced image charge move adiabatically with the electron or hole if the response time is fast compared to the band width of the quasi particles. These are electronic polarons